



Faculty of Biosciences, Fisheries and Economics

Department of Arctic and Marine Biology

Seasonal abundance and activity of sympagic meiofauna in Van Mijenfjorden, Svalbard

Vanessa Pitusi

BIO-3950 - Master Thesis in Marine Ecology – May 2019



Supervisors: Professor Rolf Gradinger¹
Associate Professor Janne E. Søreide²

Advisors: Dr. Miriam Marquardt¹

¹UiT, The Arctic University of Norway, 9019 Tromsø, ²UNIS, The University Centre in Svalbard, 9171 Longyearbyen



Table of content

Abstract	iv
Abbreviations	v
Acknowledgements	vi
1. Introduction	1
<i>1.1 Sea ice as a habitat in the Arctic</i>	1
<i>1.2 Sympagic-pelagic-benthic coupling</i>	2
<i>1.3 Molecular tools to identify sympagic fauna</i>	4
<i>1.4 Changing ice conditions in the Arctic</i>	5
<i>1.4.1 Implications of changing ice conditions on Arctic coastal ecosystems</i>	6
2. Aim of this thesis	9
3. Materials and methods	11
<i>3.1 Study site and sampling</i>	11
3.2 Collection of samples.....	12
<i>3.2.1 Sampling of ice cores</i>	12
<i>3.2.2 Sampling of microzooplankton</i>	12
<i>3.2.3 Sampling of sediment</i>	13
3.3 Sample processing	13
<i>3.3.1 Abiotic parameters</i>	13
<i>3.3.2 Chlorophyll a measurements</i>	13
<i>3.3.3 Sympagic meiofauna abundance and vertical distribution</i>	14
<i>3.3.4 Microzooplankton abundance</i>	14
<i>3.3.5 Sediment sample analysis</i>	15
3.4 Data handling	15
<i>3.4.1 Brine salinity and volume</i>	15
<i>3.4.2 Chlorophyll a calculations</i>	15
<i>3.4.3 Sympagic meiofauna abundance and vertical distribution</i>	16
<i>3.4.4 Integrated microzooplankton abundance</i>	16
<i>3.4.5 Sympagic meiofauna-environmental correlations</i>	17
3.5 Polychaete growth experiment.....	17
<i>3.5.1 Field collection</i>	17
<i>3.5.2 Growth experiment set-up</i>	18

3.5.3 Experiment data evaluation	19
3.6 DNA extraction.....	19
3.6.1 Pre-DNA extraction	19
3.6.2 DNA extraction	20
3.6.3 Pre-PCR preparation.....	20
3.6.4 PCR.....	21
3.6.5 Gel electrophoresis	22
3.6.6 Post-PCR – SPRI cleaning.....	22
3.6.7 Sanger sequencing preparation	22
3.7 Sanger sequence data processing	23
3.7.1 Cleaning of Sanger sequences	23
3.7.2 Construction of phylogenetic trees	23
4. Results	24
4.1 Environmental parameters.....	24
4.1.1 Snow depth, ice thickness, and freeboard	24
4.1.2 Sea ice physics	27
4.2 Chlorophyll a concentration – ice and water	30
4.3 Sympagic meiofauna	33
4.3.1 Temporal difference	33
4.3.2 Spatial difference	34
4.3.3 Sympagic meiofauna-environmental correlations	35
4.4 Microzooplankton abundance.....	36
4.5 Size of sea ice nematodes and polychaetes collected from the ice and during experiments.....	37
4.5.1 Nematodes.....	37
4.5.2 Polychaete juveniles.....	38
4.6 Polychaete growth experiment.....	39
4.7 Molecular data.....	42
4.7.1 Nematodes.....	42
4.7.2 Polychaete juveniles.....	43
5. Discussion	44
5.1 Sea ice as a reproductive and nursery ground.....	44
5.2 Spatial differences in sympagic meiofauna abundance	47
5.3 Sympagic-pelagic coupling in Van Mijenfjorden.....	50

<i>5.4 Molecular identification of nematodes</i>	50
6. Uncertainties and future work	52
7. Conclusion and outlook	54
Appendix A	56
Appendix B	60
Bibliography	65

Abstract

The importance of landfast ice as a nursery and breeding ground for Arctic marine invertebrates was studied in Van Mijenfjorden (77°N, 15/16°W), southwestern Svalbard from March to May 2017. The collection of first-year ice cores with stations along a depth gradient allowed the investigation of both temporal and spatial differences in sympagic meiofauna community composition and abundance. Furthermore, water column samples were retrieved to examine the strength of sympagic-pelagic coupling. Overall, 13 taxa were identified from the ice and 15 taxa from the water column with low abundances of dominant ice fauna in the water samples. Total sympagic metazoan abundance peaked in late April with over 25,000 ind m⁻², due to the reproduction of ice-associated nematodes. Throughout spring the presence of sexually mature nematodes and eggs supported the notion that sea ice in Van Mijenfjorden, especially at the main station (vMF/Mn – 50 m water depth), served as a breeding and reproductive ground to ice nematodes. Comparatively, through tight sympagic-benthic coupling, in late April, higher abundances of juvenile polychaetes (7,661 to 8,900 ind m⁻²), in the lowermost 10 cm of the ice, were recorded at the innermost stations (2 - 14 m water depth), compared to deeper stations (> 50 m water depth) (0 to 865 ind m⁻²). They were utilizing the sea ice as a nursery ground and refuge from predators. Higher growth rates and faster development of polychaete juvenile morphological features indicative of maturation were observed *in situ*, as well as in a growth experiment that mimicked natural ice algae concentrations. Conclusively, ice nematodes and juvenile polychaetes inhabited the sea ice in Van Mijenfjorden to exploit the highly concentrated ice algae located in the lowermost three centimeters of the ice for reproduction and growth.

Molecular tools revealed that all sympagic nematodes, apart from one individual from Wahlenbergfjorden (Nordauslandet, Svalbard), belong to the genus *Halomonhystera* and the family Monhysteridae, which are known from sea ice habitats. Juvenile polychaetes belonged to the family Spionidae, which is known to reside in sea ice in other parts of the Arctic.

Keywords: Sympagic meiofauna - Sea ice – Nursery ground - Molecular identification – Svalbard

Abbreviations

FYI – First-year ice

MYI – Multi-year ice

WSC – West Spitsbergen Current

AtW – Atlantic Water

ArW – Arctic Water

ESC – East Spitsbergen Current

FSW – Filtered seawater

SD- Snow depth

IT- Ice thickness

FB – Freeboard

vMF/Ref or vMF X- Van Mijenfjorden reference station (2 m water depth)

vMF/IM - Van Mijenfjorden intermediate station (14 m water depth)

vMF/Mn or vMF B – Van Mijenfjorden main station (50 m water depth)

vMF1 or vMF C - Van Mijenfjorden station 1 (78 m water depth)

vMF2 - Van Mijenfjorden station 2 (61 m water depth)

vMF30 or vMF A – Van Mijenfjorden station (30 m water depth)

GF/F – Glass fiber filter

DNA – Deoxyribonucleic acid

rDNA – Ribosomal deoxyribonucleic acid

PCR – Polymerase chain reaction

MM – Master mix

SPRI - Solid Phase Reversible Immobilization

GAMM – Generalized Additive Mixed Model

K2 + G – Kimura 2-parameter model with gamma distribution

ML - Maximum-Likelihood

MP - Maximum-Parsimony

PAR – photosynthetic active radiation

Acknowledgements

Herewith, I would like to sincerely thank both my supervisors Rolf Gradinger and Janne E. Søreide for their supervision and for giving me the opportunity to work with them. Without you I would not have been able to realize this project and I would definitely not have discovered my love for (sympagic) meiofauna. I am grateful to Jozef Wiktor for helping me learn more about protozoa and algae, which turned out to be highly abundant in my samples.

A big ‘thank you’ to Eva Leu for letting me be part of the FAABulous project (RiS-project 10383) – what an experience it has been. I have learnt much about planning and carrying out fieldwork, whilst having a lot of fun.

For my molecular work, I received help and advice from Miriam Marquardt, Tove M. Gabrielsen, Brandon Hassett and Marie Davey, which I am incredibly grateful for.

‘Thank you’ to Michael Greenacre for your assistance with the statistical evaluation of the polychaete juvenile growth experiment.

Thank you to my fellow master students and work colleagues (especially Héléna Cuny, Ane Cecilie Kvernvik, Sander Verbiest, Magnus Heide Andreassen and Margot Nyeggen) that made long days and nights in the field, laboratory and office entertaining!

My research was funded by the Norwegian Research Council (RiS-ID 10641 and 10907). Additionally, I received financial support from the UiT/Tromsø Research Foundation ArcticSIZE (project number 01vm/h15), the FAABulous project (RiS-project 10383), and the Fram Centre (Tromsø) – project EcoCice.

Vanessa Pitusi

Longyearbyen, May 2019

1. Introduction

1.1 Sea ice as a habitat in the Arctic

Sea ice is a ubiquitous feature in the Arctic. Landfast ice is commonly observed in Arctic fjords from winter to summer. Brine channels (< 2 μm to 1 mm), that form during the formation of sea ice through the expulsion of salt from the freshwater lattice (Maykut 1985), offer living space to a specialized sympagic (“ice-associated”) community (Horner et al. 1992). Sea ice harbors numerous bacteria, over 1000 species of ice algae, various protozoans and metazoans, such as ciliates, nematodes, benthic juvenile polychaetes and predacious cnidarians (Bluhm et al. 2018) (Figure 1). Sympagic meiofauna that inhabit first-year ice (FYI), such as landfast ice, is thought to originate from the pelagic and benthic realm. They utilize the ice as a nursery, feeding and breeding ground (Marquardt et al. 2011; Bluhm et al. 2018). Consequently, it is assumed that they actively migrate into the ice, whereas for rarer occurring fauna it could be argued that they are scavenged during ice formation (Carey and Montagna 1982).

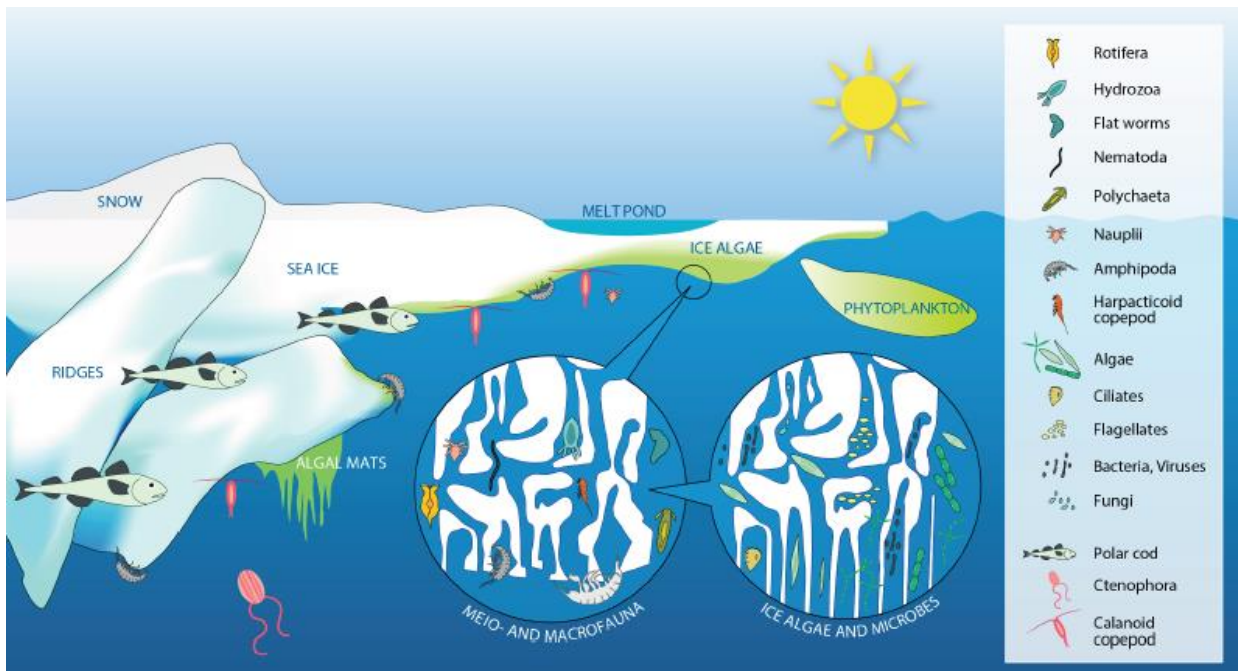


Figure 1. Sea ice as a habitat in Arctic waters. Brine channels offer a unique habitat to specialized sympagic flora and fauna (Bluhm et al. 2017).

Vertical distribution of sympagic meiofauna is influenced by a wide range of abiotic (e.g. brine salinity) and biotic (e.g. food availability) factors (Friedrich 1997), including the geometry of the brine channels (Krembs et al. 2000). The inhabitable space, the brine volume, is determined by the *in situ* ice temperature and bulk salinity of the ice. The most stable conditions are found at the ice-water interface and thus the majority of sympagic flora and fauna are concentrated in the lower 10 cm of the ice sheet (Friedrich 1997).

Microscopic algae that live within the ice, predominantly diatoms, offer an early and concentrated food source to organisms after the dark and unproductive winter (Horner and Schrader 1982; Sørense et al. 2010; Leu et al. 2015). Ice algae play a vital role in the sympagic realm and it has been estimated that they can contribute up to a third of the total annual primary production in the Arctic Ocean (Mundy et al. 2005). Additionally, they couple the sympagic realm to the pelagic and benthic domain (Gradinger 1999a). Ice algal growth is controlled primarily by abiotic factors (e.g. light and snow cover) and commences as soon as light intensity increases after the polar night (Leu et al. 2015). At the start of spring, sea ice chlorophyll *a* concentrations are low and the ice community is predominantly heterotrophic (Figure 2). As the day length and solar angle increases, light becomes more readily available and ice algae start to grow exponentially (Gradinger 1999a). Chlorophyll *a* concentrations within the ice tend to peak in late April to early May in the lower 10 centimeters of the ice sheet, depending on environmental condition. The last stage is the release of ice algal biomass to the water column and benthos due to ice melt as a consequence of warmer atmospheric and potentially water temperatures (Leu et al. 2015).

Although sympagic meiofaunal groups are known to be predominantly herbivorous, their grazing does not limit ice algal biomass in sea ice (Gradinger 1999b; Michel et al. 2002). However, grazing ice algae allows for development and growth in early spring before the phytoplankton bloom commences (Sørense et al. 2010).

1.2 Sympagic-pelagic-benthic coupling

The flow of energy, flora, and fauna between the sea ice, water column and seafloor is known as sympagic-pelagic-benthic coupling. Various factors, such as bottom depth, influence the strength of this coupling. It has been observed that landfast ice, in Arctic marine coastal

ecosystems, with a bottom depth of less than 50 m tends to host sympagic assemblages dominated by benthic larvae and juveniles (e.g. from polychaetes) (Gulliksen and Lønne 1991; Bluhm et al. 2018). Water depths greater than 50 m tend to favor early life stages of pelagic organisms related to the decreasing abundance of meroplankton (Bluhm et al. 2018).

In early and late spring, when the microalgae that inhabit the ice are growing exponentially, they are solely accessible to in-ice fauna and pelagic organisms that can actively swim up to the underside of the ice to feed. Søreide et al. (2010) and Daase et al. (2013) established that *Calanus glacialis* relies on ice algae to fuel its growth and reproduction in early spring to ensure a match between the phytoplankton bloom and nauplii hatching. In addition, albeit ice algae contribute little to the overall primary production around Svalbard, Søreide et al. (2013) showed that both pelagic and benthic organisms are dependent on sea ice algae. Especially, benthic larvae (e.g. polychaete juveniles) rely on ice algae in spring to fuel growth and development (e.g. McConnell et al. 2012). Later in the season, when sea ice is starting to melt, sympagic-benthic coupling becomes stronger as ice algae are flushed out of the ice and start sinking through the water column faster than they can be scavenged (Leu et al. 2015) (Figure 2).

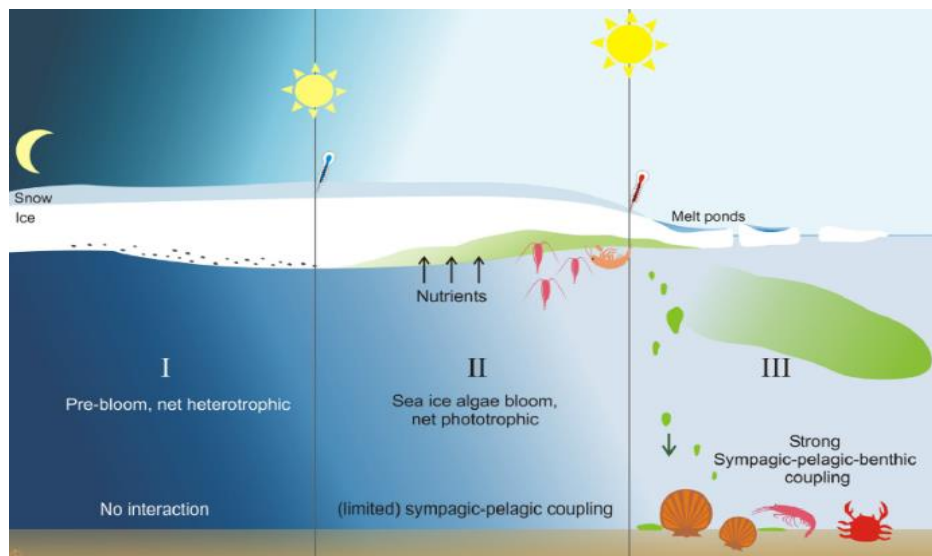


Figure 2. Development of ice algae throughout spring in ice-covered waters and the strength of coupling to the pelagic and benthic realm (taken from Leu et al. 2015).

1.3 Molecular tools to identify sympagic fauna

Few species are known from the sympagic realm due to the lack of taxonomic keys and the cryptic nature of the organisms that inhabit sea ice. Without in-depth taxonomic knowledge and electron microscopes, it is difficult to assign a species name to the meiofauna found and to determine their ecological role in the marine Arctic coastal system.

Free-living nematodes are one of the most abundant meiofauna groups in fresh- and seawater environments (Heip et al. 1985; Moens and Vincx 1997). Additionally, free-living nematodes are known to numerically dominate sympagic communities in spring before the summer melt (e.g. Horner et al. 1992; Marquardt et al. 2011). Nematodes play an important role in connecting primary producers to higher trophic levels by serving as a food source to pelagic and benthic macrofauna (Vranken 1987; Majdi and Traunspurger 2015), and by directly influencing bacterial communities (De Mesel 2006; Majdi and Traunspurger 2015); both positively and negatively. The first description of sympagic nematodes came from Tchesunov (1986) from Arctic pack ice – *Theristov melnikovi*. Since then two more species have been described by Tchesunov and Riemann (1995) – *Cryonema crissum* and *C.tenua*. However, no further studies have been conducted to identify nematodes from sea ice. The described ice nematodes belong to the highly successful family Monhysteridae, which is well-represented in the marine environment by seven genera and 70 species, of which all are believed to be associated with the seafloor (Fonseca and Decraemer 2008).

It has been estimated that only a small fraction of the “real” nematode diversity has been studied so far (e.g. Bhadury et al. 2006; Derycke et al. 2007a). Due to their small size and cryptic nature, identifying nematodes morphologically is time-consuming. Morphological descriptions of marine nematodes are sparse and often published in not easily accessible scientific journals (Fonseca and Decraemer 2008). Subsequently, the use of molecular tools (e.g. 18S rDNA and COI gene) has become increasingly popular (e.g. Derycke et al. 2010a; Brandner et al. 2016; Marquardt et al. 2018) in order to identify cryptic fauna to the lowest taxonomic level possible, and to reveal high taxonomic diversity even over small scales (e.g. Derycke et al. 2007a).

Both Piraino et al. (2008) and Marquardt et al. (2018) used molecular tools to identify the sympagic hydrozoan *Sympagohydra tuuli*, enabling the identification of a new species and its pan-Arctic distribution.

1.4 Changing ice conditions in the Arctic

Over the past three decades, the Arctic has experienced a more significant increase in both its sea surface and air temperatures, compared to anywhere else (Comiso et al. 2008; Screen and Simmonds 2010a; Gjelten et al. 2016).

As a result, sea ice cover has decreased by approximately 40 % and is slowly changing from a multi-year ice (MYI) dominated ocean to a FYI dominated region (Comiso 2012; Stroeve et al. 2014). In 1979, sea ice extent ranged from 7 to 14 x 10⁶ km² (Walsh and Johnson 1979) compared to the summer minimum and winter maximum recorded in 2017 with 4.82 to 13.76 x 10⁶ km² (NOAA 2019) (Figure 3). Not just the age of the sea ice is changing. In addition to becoming younger, the ice is getting progressively thinner, saltier, less deformed and snow-covered (Nicolaus et al. 2012).

Overall, sea ice loss has been more severe than predicted by models, especially in Arctic fjords (Muckenhuber et al. 2016), likely as a consequence of a positive feedback loop between the melting sea ice and fraction of open water (known as Arctic amplification). Sea ice has a high albedo that reflects most of the incoming shortwave radiation. As a result of changing precipitation and ultimately less snowfall (Screen and Simmonds 2012), more light and thus heat is being transmitted into the underlying ocean. Seawater acts as a dark body and absorbs incoming radiation, increasing its heat budget. This augmented input of heat leads to an earlier onset of sea ice melt (Nicolaus et al. 2012), as well as a lengthened melt season (Stroeve et al. 2014).

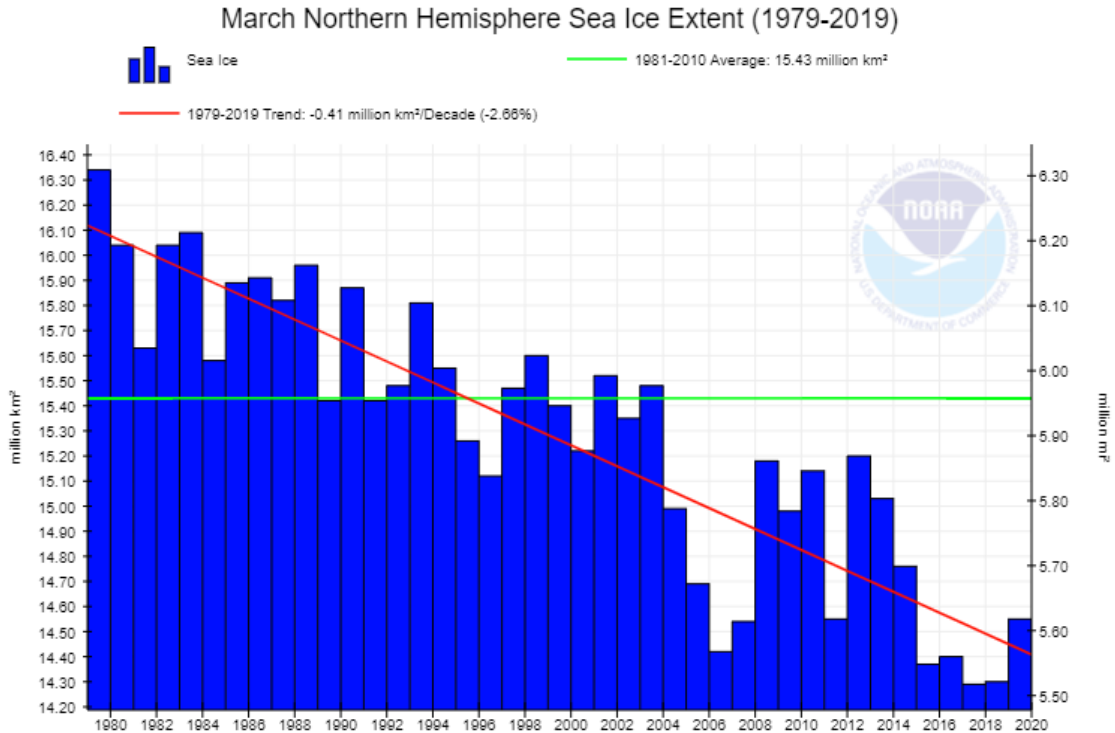


Figure 3. Arctic sea ice extent from 1979 – 2019 with trend lines (NOAA, 2019).

Of all Arctic regions, Svalbard has experienced some of the most severe temperature increases (e.g. Nordli et al. 2014), with warmer winter temperatures and subsequent FYI loss, especially in winter (Isaksen et al. 2016). Total failure of sea ice formation has occurred in Isfjorden and even fjords considered to be more Arctic have not been unaffected (e.g. Van Mijenfjorden). Changes in wind-driven currents are pushing progressively more warm Atlantic Water (AtW) onto the shelf and into western Spitsbergen fjords, resulting in warmer seawater temperatures and a lack of sea ice formation (Muckenhuber et al. 2016; Nilsen et al. 2016). Atmospheric temperatures are also on a rise (Gjelten et al. 2016; Isaksen et al. 2016), meaning that seawater is not able to lose sufficient heat during the winter to facilitate sea ice formation.

1.4.1 Implications of changing ice conditions on Arctic coastal ecosystems

Changing sea ice conditions will have implications on the stratification, light regime, temperature, as well as primary and secondary production, of the underlying water column (Søreide et al. 2010). It has been speculated that there will be a shift in the coupling between the sympagic-pelagic-benthic realm. Less and thinner sea ice will reduce the strength of sympagic-

benthic coupling, but enhance sympagic-pelagic interactions (Eamer et al. 2013). There might be a reduction in the vertical flux of particulate organic matter (Hunt et al. 2016), which will affect benthic communities and their productivity.

Thinner, less snow-covered sea ice means that light will become more available and earlier, in a system that previously has been characterized by at least four months of darkness, or even up to six months in ice-covered waters (Berge et al. 2014). Increased input of light will have a pronounced effect on Arctic primary producers. Under-ice phytoplankton blooms might become a more common occurrence (Arrigo et al. 2012; Assmy et al. 2017) and food availability to pelagic grazers might increase. However, earlier sea ice algal and phytoplankton blooms might have negative implications and potentially leading to a mismatch between primary and secondary producers (Søreide et al. 2010).

Additionally, increased freshwater input from rivers and glacial melt (Peterson et al. 2006; Hunt et al. 2016), will transport more terrigenous material into Arctic marine coastal systems. This will not only impact sympagic fauna (Gradinger et al. 2009), but the pelagic (Søreide et al. 2010) and benthic (Renaud et al. 2007) realm as well.

However, it is difficult to assess these changes without a sufficient database on the organisms that inhabit these realms. Most importantly, it is essential to determine whether sea ice plays a vital role in the life cycle of pelagic and benthic fauna in order to assess which of the proposed changes might become reality.

1.5 An archipelago in the Arctic - Svalbard

Svalbard is an island group located between 74° and 81°N with the Fram Strait to the west, the Barents Sea to the south-east and the Arctic Ocean to the north. The largest island is called Spitsbergen, which is influenced by warm, saline (> 3°C, > 34.9) Atlantic water (AtW) to the west and cold, fresh (< 1 °C, 34.3 - 34.8) Arctic water (ArW) to the east (Cottier et al. 2005). The ArW flows as the East Spitsbergen Current (ESC) close to the coast from the east to the west and in the past has shielded fjords from the intrusion of AtW (Figure 4).

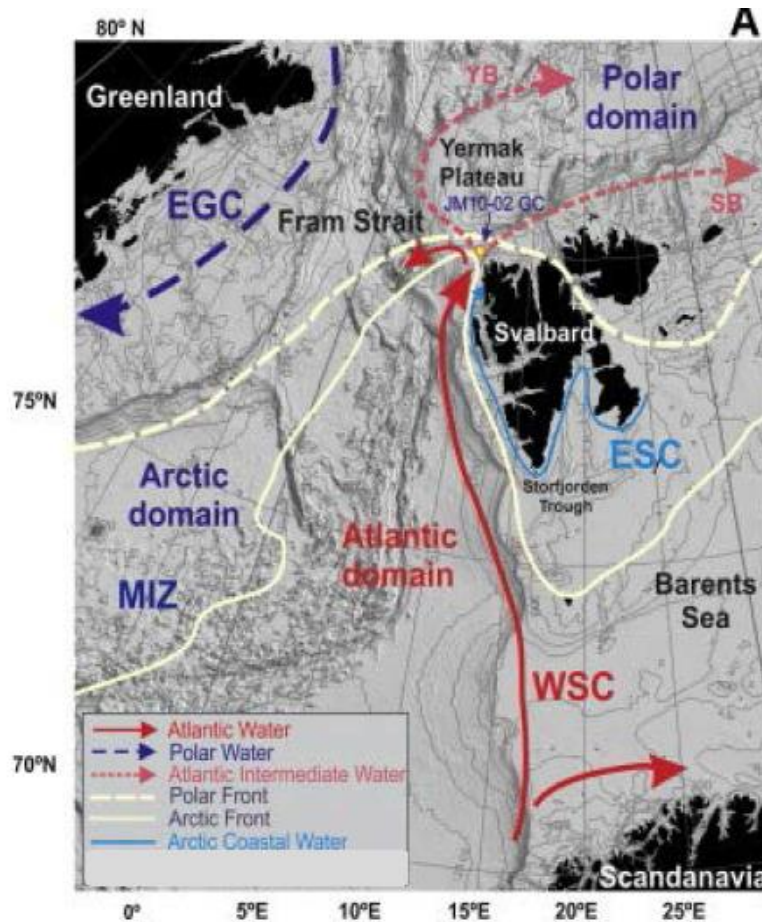


Figure 4. Map of the two main currents around Svalbard that influence the formation of sea ice and other process in the marine environment (taken from Chauhan et al. 2014).

60 % of Spitsbergen is covered in glaciers and characterized by its many fjord systems, of which several have glacier fronts at the end. Subsequently, local water production is another factor influencing sea ice formation.

The average winter air temperature on the west coast of Spitsbergen is -15°C , which is relatively warm for the Arctic. Subsequently, seasonal sea ice cover varies depending not only on ocean circulation but also atmospheric forcing.

Due to its northern location, Svalbard has an extreme light environment with four months of darkness in winter and four months of sunlight in the summer. In ice-covered fjords, this period might be up to two months longer than in ice-free systems (Berge et al. 2014). Consequently, organisms have to be adapted to these light conditions and able to respond quickly to changing environmental conditions to ensure successful reproduction and development. Although, sea ice studies around Svalbard exist most of them focus on the physics of either FYI or pack ice, but

only a few studies exist investigating the biological aspect of sea ice and its coupling to the rest of the Arctic marine coastal ecosystem (e.g. Søreide et al. 2010; Leu et al. 2011).

2. Aim of this thesis

This master thesis was created to obtain more in-depth knowledge about the ecology of sympagic meiofauna abundance and activity on Svalbard, based on the insights gained from Pitusi (2016). Studies on landfast ice exist from the Canadian Arctic and along the coastline of Alaska, but little focus has been put on the importance of seasonal landfast ice as a nursery ground to meroplankton and a reproductive ground to adult zooplankton. Numerous of the publications focus on identifying sympagic meiofauna communities and diversity, which adds valuable information, but fails to specify the importance of landfast ice to pelagic and benthic organisms, in coastal marine Arctic ecosystems. Studies investigating the importance of landfast ice as a breeding ground and refuge for meroplankton are urgently needed in the light of changing ice conditions. Both failure of sea ice formation and early ice break-up will have consequences on the light regime, stratification, temperature and biological processes, of the underlying water column (Søreide et al. 2010). Unfortunately, it is difficult to assess the impact of these changing sea ice conditions on the Arctic coastal ecosystem without a sufficient database. This study aims shed some light onto the activity of sympagic meiofauna in spring, and to contribute towards the establishment of a broader database on sea ice ecology in the European Arctic, which is poor to this date.

The main hypothesis of this study was as followed:

Is sea ice in Van Mijenfjorden an important reproductive and nursery ground for pelagic and benthic organisms?

The following sub-goals were added in order to help answer the main hypothesis of this project.

- 1. How does sympagic meiofauna abundance and community composition vary along a depth transect?*

To investigate this objective, a depth transect with five ice sampling stations was created along the axis of Van Mijenfjorden (Figure 5). The hypothesis is that with increasing bottom depth, the sympagic communities will be increasingly dominated by pelagic rather than benthic organisms.

2. *Does meiofauna abundance in the water column compare to that of sea ice?*

The microzooplankton community (including meroplankton) was examined to determine the potential for sympagic-pelagic-benthic coupling in Van Mijenfjorden along the depth transect.

3. *Are growth rates of juvenile polychaete larvae higher at ice algae concentration compared to phytoplankton concentrations in spring?*

Polychaete juveniles are well-known components of sympagic communities all over the Arctic, especially in landfast ice. Although they are highly abundant in sea ice and the underlying sediment, little is known about their complete life cycle. In order to determine whether juvenile polychaetes require sea ice and the highly concentrated ice algae to grow, a growth experiment with four different food concentrations was conducted.

4. *Can molecular tools be used to increase the taxonomic resolution of identifying sympagic meiofauna?*

The database for sympagic meiofauna is sparse, especially for Svalbard. Bluhm et al. (2018) compiled all available sympagic meiofauna data on a pan-Arctic scale, but in-depth identification of these organisms is still lacking. It is time-consuming work that requires skill due to the cryptic nature of meiofauna. This thesis aims to identify the most dominant sympagic meiofauna to the lowest taxonomic level possible through the use of molecular tools.

These research questions were addressed through extensive field- and laboratory work carried out in spring 2017 through to autumn 2018.

3. Materials and methods

3.1 Study site and sampling

Van Mijenfjorden is a partially enclosed fjord with an island (Akseløya) at its mouth, on the southwest coast of Spitsbergen (Svalbard). The 70 km-long fjord and consists of an inner and outer basin with average depths of 30 and 100 m (Høyland 2009), respectively. Riverine input, sea ice, and glacial melt influence the hydrography. Van Mijenfjorden is one of the last west Spitsbergen fjords where parts are still seasonally covered by fast ice. Sea ice starts forming around January/February and melts around May/June.

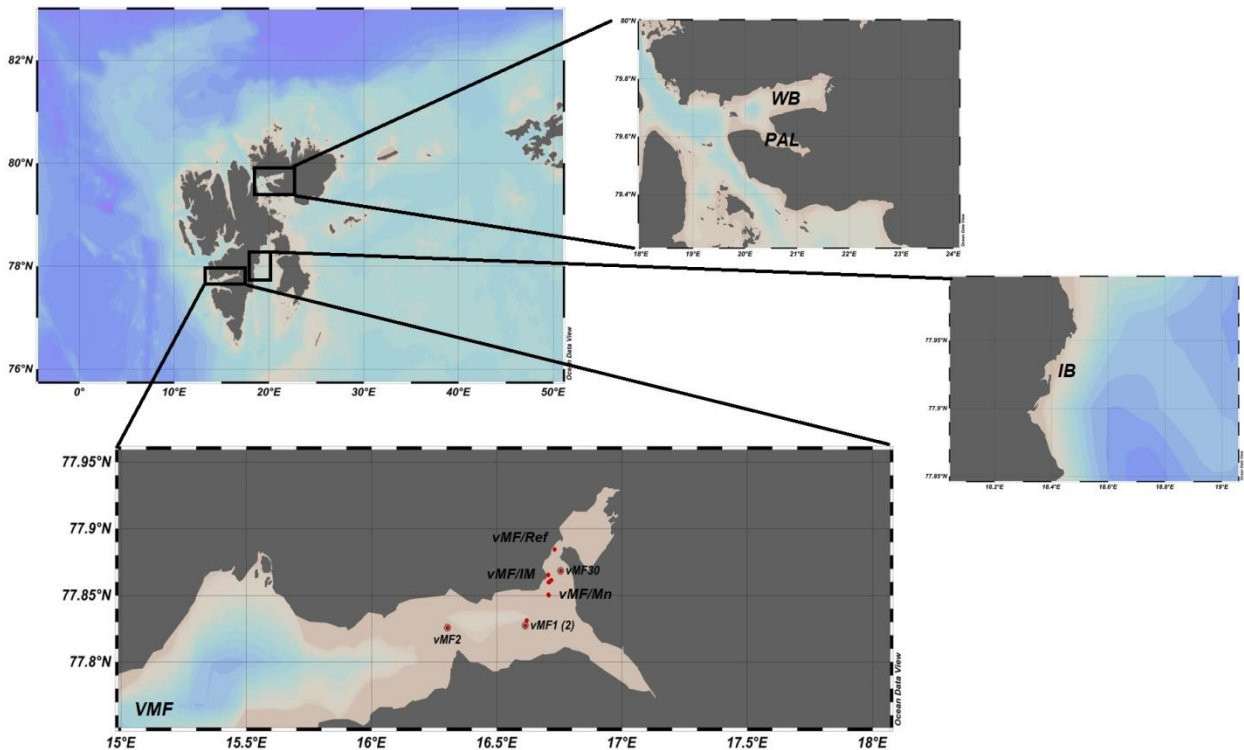


Figure 5. Map of all sampling locations around Svalbard, where VMF = Van Mijenfjorden, WB = Wahlenbergfjorden, PAL = Palanderbukta and IB = Inglefieldbukta.

Sampling of landfast ice and the underlying water column took place from March to May 2017 at five stations along a depth transect (2 – 78 m) in Van Mijenfjorden (Figure 5). In 2018, a selected sub-set of stations was re-visited to collect material for polychaete juvenile growth experiments.

Additionally, sea ice samples were collected from the east coast of Svalbard (Table A1) and a two-day cruise, onboard of *MS Polarsysssel*, took place in November 2018 during which water and sediment samples were collected at previously established stations (Table A2).

3.2 Collection of samples

3.2.1 Sampling of ice cores

Full sea ice cores were collected for sympagic meiofauna abundance and vertical distribution. Additionally, cores for *in situ* ice temperature, bulk salinity and chlorophyll *a* biomass were taken from undisturbed ice. A hand-held KOVACS ice corer ($\phi = 9$ cm) was used to collect ice cores. At each stations, snow depth, ice thickness, as well as freeboard were measured (Table 1). Positive freeboard was recorded when the water line was below the ice edge, whereas negative freeboard is defined as water on top of the ice.

For every station, one whole ice core and two to three replicates of the lower 10 cm were extracted. The ice cores were cut into sections of 0-1, 1-2, 2-3, 3-10 cm and every 10 cm. These distances are measured from the ice-water interface. The sections were stored in plastic bags and 100 mL of GF/F filtered seawater (FSW) per centimeter ice thickness was added to prevent osmotic shock of sympagic flora and fauna (Garrison and Buck 1986; Spindler and Dieckmann 1986); the exceptions were the cores used for bulk salinity measurements. Ice cores for biotic parameters were shielded from sunlight to avoid photodegradation of material. All samples were melted in the dark.

3.2.2 Sampling of microzooplankton

A 20 μm net (Hydro BIOS, Germany, $\phi = 40\text{cm}$) was used to collect zooplankton samples in April and May 2017 through a hole in the ice (Table 1). The net was lowered through the water column to approximately 5 m above the bottom and then pulled up no faster than 1 m s^{-1} to the surface. The samples were transferred from the cod end to a 250 mL pre-labelled sampling bottle and preserved in either 70-96 % ethanol or 4 % formalin.

In 2018, two 20 μm net zooplankton were collected alongside sediment sample at three stations – one fixed with ethanol and one fixed in formaldehyde (Table A2).

3.2.3 Sampling of sediment

A large Van Veen grab (0.1 m²) was used to collect sediment samples at three different stations (vMF A, B, C) in November 2018. A small hand-held Van Veen grab (0.025 m²) was used to retrieve a sample at station vMF/Ref (or vMF X). Water depths at the stations varied between 0.8 and 79 m.

After successful sampling, the windows atop the grab were used to take note of the colour, texture, and smell of the sediment, and the fullness of the grab. All four windows were opened and four times the top 3 cm of sediment were randomly taken from the grab sample with a plastic syringe ($\varnothing = 2.6$ cm). This process was repeated twice – once for ethanol and formaldehyde preservation. The collected samples were passed firstly through a 500 μm sieve and secondly through a 63 μm sieve, after which it was transferred to a pre-labelled 250 mL sampling bottle. The rest of the sample was emptied into a black tub and broken up to expose any macrofauna sitting in the sediment. This fauna was preserved in a separate pre-labelled 250 mL sampling bottle and filled with pure ethanol.

3.3 Sample processing

3.3.1 Abiotic parameters

In situ ice temperature was measured directly after the extraction of the core with a hand-held thermometer (*VWR Traceable Digital Thermometer*, VWR, USA) by placing it in pre-drilled holes at 0, 1, 2, 5 cm and every 10 cm intervals.

The bulk salinity of the cores was determined after melting with a conductivity meter (*VWR symphony SP90M5 Handheld Meter with Electrode salinity probe*, VWR, USA). The brine salinity and brine volume fraction were calculated using the calculation provided by Cox and Weeks (1983).

3.3.2 Chlorophyll *a* measurements

The volume of each melted section was measured prior to vacuum filtration through 0.7 μm GF/F glass fiber filters (Whatman, England). Chlorophyll *a* analysis followed Vader et al. (2014) with slight changes in the methodology.

All samples were stored in a -80°C freezer after filtration. For analysis, the filters were thawed and stored in 10 mL methanol for no longer than 24 hours at 4°C in the dark. Fluorescence was analyzed with a previously calibrated *F10-AU Fluorometer* (Turner, USA).

A blank reading with pure methanol was determined prior to each chlorophyll *a* measurements. Samples that displayed readings that were too high were diluted with methanol. After an initial reading was taken, two drops of 10 % HCl were added to degrade any remaining chlorophyll *a*, and fluorescence was again measured to calculate the phaeopigments concentrations. Corrected chlorophyll *a* concentrations were calculated after McMinn et al. (2009).

3.3.3 Sympagic meiofauna abundance and vertical distribution

The total volume for each melted meiofauna core section was measured and the sample was passed through a 20 µm sieve. Concentrated samples were analyzed using a Leica stereomicroscope (*Leica M16*, Wetzler, Germany). The fauna was identified, counted and preserved in 70-96 % ethanol for molecular analysis. Photos were taken of the individuals taken for DNA extraction, where possible.

General taxonomic literature (e.g. Larnik and Westheide 2011), was used to identify organisms to the lowest taxonomic level possible. No identification key for eggs was available and thus note of their width and colour was made, and photographs were taken to establish a catalogue.

3.3.4 Microzooplankton abundance

Net samples were concentrated in a 20 µm sieve under a fume hood and washed in GF/F FSW for 30 mins. The washed sample was diluted in a known volume in a beaker and sub-samples of either 2 or 5 mL were taken, depending on the density of the sample. A total of 300 individuals was counted per sample using a Leica stereomicroscope (*Leica M16*, Wetzler, Germany). The remaining complete sample was scanned for any rare species.

3.3.5 Sediment sample analysis

The ethanol-fixed sediment samples were concentrated over a 63 µm wire sieve and washed in GF/F FSW for 30 mins. The washed sample was transferred to a petri dish and scanned through using a Leica stereomicroscope (*Leica M16*, Wetzler, Germany). The desired organisms were nematodes and juvenile polychaetes. Approximately 10 nematodes, of different morphology, were picked from each station and at least five polychaetes. The specimens were washed three times in MilliQ water and placed, with as little liquid as possible, in 2 mL Eppendorf tubes (Eppendorf, Germany). They were placed in the -80°C freezer until DNA extraction.

3.4 Data handling

Data handling consisted of calculations for various variables (e.g. brine salinity and ice algal biomass), data visualization and statistical analysis. Figures were created with *R V 3.4* (R Core Team 2017) and *R* package *ggplot2* (Wickham 2009).

3.4.1 Brine salinity and volume

The brine salinity and volume were calculated based on the equations from Cox and Weeks (1983).

$$\text{Brine salinity} = 1000 / (1 - (54.11 / \text{in situ ice temperature})) \quad (\text{Eq.1})$$

$$\text{Brine volume (\%)} = \text{Bulk salinity} * (0.0532 - (4.919 / \text{in situ ice temperature})) \quad (\text{Eq.2})$$

3.4.2 Chlorophyll *a* calculations

Corrected chlorophyll *a* concentrations were calculated based on McMinn et al. (2009). The following equations were used:

$$\text{Chlorophyll } a \text{ } [\mu\text{g/L}] = (\text{Chlorophyll } a \text{ read out} - \text{Phaeophytin read out}) * 1.7 * (\text{Methanol volume [mL]} / \text{Volume filtered [mL]}) * \text{Dilution factor} \quad (\text{Eq.1})$$

Where 1.7 is a constant obtained from the calibration of the fluorometer.

In order to convert the chlorophyll *a* concentration over the area of each ice core section, this calculation was used:

$$\text{Chlorophyll } a \text{ [mg m}^{-2}\text{]} = \text{Chlorophyll } a \text{ [\mu g/L]} * \text{height of core section [m]} \text{ (Eq.2)}$$

3.4.3 Sympagic meiofauna abundance and vertical distribution

The abundance of sympagic meiofauna was calculated for each section of the ice core was calculated after Bluhm et al. (2018):

$$\text{Sympagic meiofauna abundance [ind m}^{-2}\text{]} = \frac{1000 * C * h * n}{V} \text{ (Eq.1)}$$

Where *C* is the ice volume correction factor (0.92 - based on ice density after Timco and Frederking 1996), *n* is the number of sympagic meiofauna in a section, *h* is the height of the core section in meters, and *V* is the pure ice volume of the melted section in liters.

3.4.4 Integrated microzooplankton abundance

Microzooplankton abundance was calculated using Equations 1 to 3. Firstly, the fraction counted had to be determined (Eq.1), as mostly sub-samples rather than the whole sample were counted.

$$\text{Fraction counted} = \text{Total sample volume (mL)} / (\text{Number of sub-samples} * \text{Sub-sample volume (mL)}) \text{ (Eq.1)}$$

From the fraction counted, the number of individuals per sample was calculated using Equation 2.

$$\text{Number of individuals per sample} = \text{Fraction counted} * \text{Total number of individuals counted} \text{ (Eq.2)}$$

Abundance of individuals per m^2 in the net samples was calculated using Equation 3.

$$\text{Abundance net samples (ind } m^{-2}) = \text{Number of individuals per sample/Net mouth opening (} m^2) \quad (\text{Eq.3})$$

3.4.5 Sympagic meiofauna-environmental correlations

Based on the trends shown in Bluhm et al. (2018) between environmental parameters and individual groups of sympagic meiofauna, data from the main station (vMF/Mn) and transect (26 to 30 April) were used to test correlations between variables and metazoan abundance, in the lowermost 10 cm of the ice. The environmental variables tested were chlorophyll *a*, Julian day, solar angle and water depth. Using *R V 3.4* (R Core Team, 2017) a Spearman's rank correlation test was performed to test these correlations. In addition, these tests were performed for just nematodes and total sympagic meiofauna abundance, in the 0-1 and 0-3 cm section, for station vMF/Mn due to the strong gradients in abundance between ice sections.

Correlations that were of interest based on trends observed in literature (e.g. polychaete juvenile abundance and water depth) were further tested with a (Quasi) Poisson regression.

3.5 Polychaete growth experiment

From April to May 2018, a polychaete juvenile growth experiment was conducted with 115 polychaete larvae.

3.5.1 Field collection

Juvenile polychaetes of similar size and morphology were picked from qualitative landfast ice samples in Van Mijenfjorden, Svalbard. On 25 March 2018, two 1 x 1 m blocks were cut out of sea ice and the lower 5 cm were sawed off and collected in plastic bags. 1.5 L of GF/F FSW was added to the samples and they were kept in the dark until further processing.

After complete melt, the samples were concentrated over a 20 μm sieve and examined under a *Leica MZ16* stereomicroscope (Wetzler, Germany). In total, 115 polychaete juveniles were

picked from the remainder of the sample and kept in 0.7 μm FSW with natural ice algal communities in an incubator at 2°C.

For the experiment, a monoculture of *Nitzschia frigida* (one of the most abundant sea ice diatoms at the stations) was used to make food stocks at different cell abundances (Table A3) in order to mimic natural chlorophyll *a* concentrations found in the ice (see Pitusi 2016).

3.5.2 Growth experiment set-up

Four feeding concentrations were established – control (no food), low, medium and high. Initially, food concentrations were determined through chlorophyll *a* extraction (7 April 2018), but due to methanol contamination, the method was substituted for cell counting. ‘Fresh’ methanol had been inadvertently mixed with waste methanol. Subsequently, *N. frigida* cells were counted with a *Fuchs-Rosenthal* chamber counter (0.0025 m^2) (Assistant, Germany) and the volume of cultured algae needed to reach the appropriate food concentration for each treatment was calculated (Table A3).

The experiment was conducted at 0°C with a 12:12 dark and light cycle, which was tracked using three *HOBO* temperature and light loggers (Onset, USA). The juvenile polychaetes were starved 24 hours prior to the experiment by being placed in autoclaved 0.2 μm FSW at 2°C. During the experiment, the polychaete juveniles were kept in Costar 6 well-plates (VWR, USA); there was one plate for each treatment (control, low, medium, and high). Each well contained five polychaete juveniles and for all treatments, bar the control, six wells were used (Figure A1). The wells were filled in total with 8 mL of autoclaved 0.2 μm FSW with the appropriate food concentration. Every 3-5 days, the water was replaced. The number of algal cells was counted, in the morning of every food replenishing event, to ensure the correct volume of food stock was added. The polychaete juveniles were picked from the wells of each treatment and placed in a sterile petri dish. Photographs were taken of individual specimens with a SONY digital camera attached to either a *Leica MZI6* or *Leica M205C* stereomicroscope (Wetzler, Germany) at varying magnifications (7.1 – 80 x). Afterwards, the polychaete juveniles were transferred to new and sterile well-plates filled with 6 to 8 mL of autoclaved 0.2 μm FSW with the appropriate food concentration. In total, the experiment ran for 44 days.

To track growth, the number of setiger of all polychaete juveniles was determined, and note of the development of morphological features (e.g. palps) was made, from the photographs using *ImageJ V 1.52* (Rasband 2018).

3.5.3 Experiment data evaluation

The experimental data were processed using *R V 3.4* (R Core Team 2017). A Generalized Additive Mixed Model (GAMM) was used to evaluate the growth data. As the number of setiger counted over time could not be assigned to specific individual polychaete juveniles, at every food replenishing event, the aggregated mean setiger number was calculated for each well. Consequently, it was assumed that this aggregated mean value was constant over time and representative of any potential change in number of setiger. In other words, it ensured that the model could assume that the treatment might be having a direct effect on the setiger number counted over time. Using this value, a GAMM was built with the number of setiger as a response variable and the duration of the experiment (in days), well number and food treatment as predictor variables.

3.6 DNA extraction

Two different types of DNA extraction methods were used to maximize extraction success of DNA from sympagic meiofauna – *DNeasy Blood and Tissue Extraction* (Qiagen, USA) and *HotSHOT* genomic DNA preparation (Truett et al. 2000; Alassad et al. 2008).

3.6.1 Pre-DNA extraction

Prior to the extraction of DNA from selected specimens, individual organisms were washed in MilliQ water. Each individual was rinsed two to three times in MilliQ water to ensure that no or little detritus was attached to its exterior and no ethanol was left. After rinsing, each specimen was placed in a single 1.5 mL Eppendorf tube with 180 μ L ATL buffer for the *DNeasy Blood and Tissue Extraction*.

For the *HotSHOT* extraction method, organisms were placed in PCR tubes filled with 25 μ L Alkaline Lysis Buffer.

3.6.2 DNA extraction

For the extraction with the *Qiagen Blood and Tissue* kit, 20 μL of proteinase K was added to each pre-prepared Eppendorf tube, and samples were vortexed for seven seconds to mix thoroughly. The samples were incubated at 56 °C for two hours in an *Eppendorf thermomixer C* (Eppendorf, Germany) to ensure complete lysis of cells. After cell lysis, samples were vortexed for 15 seconds. Subsequently, 200 μL Buffer AL and 200 μL ethanol (96-100 %) were added separately and samples were vortexed to ensure a homogeneous solution. The mixture was pipetted into a labelled DNeasy spin column placed in a 2 mL collection tube. The samples were centrifuged for one min at 8,000 rpm, after which the flow-through was discarded. The spin column was placed into a new 2 mL collection tube and 500 μL Buffer AW1 was added. The tubes were centrifuged (*Centrifuge 5424*, Eppendorf, Germany) for one min at 8,000 rpm; the flow-through and tubes were discarded. Once again, the spin column was placed in a new 2 mL collection tube and 500 μL Buffer AW2 was added. Centrifugation for three min at 14,000 rpm followed. The flow-through and tube were discarded and the spin column was placed in a 1.5 mL Eppendorf tube to which 200 μL Buffer AE was added, in order to elute the DNA. The sample was left to incubate for 1 min at room temperature and centrifuged for 1 min at 8,000 rpm. This step was repeated by using the elute at the bottom of the tube, in order to increase DNA yield. After the second centrifugation, the spin column was discarded and the DNA yield was kept cold for PCR (Polymerase Chain Reaction) preparation.

For the *HotSHOT* DNA extraction, individual organisms in the pre-prepared PCR tubes were heated at 95°C for 30 minutes in a PCR machine. Once lysed, 25 μL Neutralization Buffer was added for stabilization; the DNA was ready for PCR.

A negative control without DNA was included, in both methods, to check for contamination.

3.6.3 Pre-PCR preparation

After the DNA extraction, a MasterMix (MM) was prepared. This consisted of 10 \times *DreamTaq Buffer* (Thermo Scientific, USA), *dNTPS* (2.5 mM), forward and reverse primers (10 μM), *DreamTaq Polymerase* (Thermo Scientific, USA), MilliQ water, which was added to DNA, a positive and negative control.

Two specific nematode primers from Bhadury et al. (2006) were used to amplify 345 bp of the 18S rDNA gene – (1) *MN18F* (forward) (5'- CGCGAATRGCTCATTACAACAGC - 3') (IDT, USA) and (2) *Nem_18S-R* (reverse) (3' - GGGCGGTATCTGATCGCC – 5') (IDT, USA).

For the polychaete DNA amplification, two specific invertebrate primers were used to target the highly variable mitochondrial COI region – (1) *mlCOLintF* (forward) (5' - GGWACWGGWTGAACWGTWTAYCCYCC – 3') (Leray et al. 2013) and (2) *lgHCO2198* (reverse) (5' – TAIACYTCIGGRTGICCRAARAAYCA – 3') (Leray et al. 2013).

Concentrations of each 'ingredient' were calculated for the correct amount of samples, meaning that each PCR tube was filled with 25 µL, of which 23 µL consisted of the MM and 2 µL DNA. The enzyme, *DreamTaq Polymerase*, was added last to reduce the risk of primer dimers from forming. Two controls were included – one positive consisting of the buffer solution with previously extracted DNA of the target organism and a negative control of MilliQ water, to which the MM was added.

3.6.4 PCR

The tubes were placed in a PCR machine (*Mastercycler egradient S*, Eppendorf, Germany) and the following cycle was programmed for nematode DNA amplification in 2017:

95 °C – 5 mins, 37 cycles x (95 °C – 1 min, 54 °C – 1 min, 72 °C – 2 min), 72°C – 5 min, 4 °C – infinite.

In 2018, the following PCR cycle was used to amplify nematode DNA:

94 °C – 5 mins, 40 cycles x (94 °C – 1 min, 54 °C – 1 min, 72 °C – 2 min), 55°C – 2 min, 72°C – 5 min, 4 °C – infinite.

The following touchdown PCR was programmed for polychaete DNA amplification:

16 x (95°C – 10 sec, 62°C – 30 sec, (minus 2°C for every 2nd cycle), 72°C – 60 sec), 25 x (95°C – 10 sec, 46°C – 30 sec, 72°C – 1 min), 72°C – 5 min, 4°C – infinite.

3.6.5 Gel electrophoresis

A large 1 % agarose gel (95 mL TAE buffer, 0.95 g agarose) was prepared and stained with *GelRedTM Nucleic Acid* (Biotium, USA), to check for PCR products. A *FastRule ladder* (Thermo Scientific, USA) was used to compare the products to, and bands were made visible under UV light with *GeneFlash 0.34* (Syngene). 3 μ L of the ladder was loaded onto the gel, in addition to 5 μ L of DNA, which was stained with a tiny drop of *6 x TriTrack DNA Loading Dye* (Thermo Scientific, USA). The gel was run at 210 V for 10 mins. Successful products were marked and the amplified DNA was cleaned using the solid-phase reverse immobilization (SPRI) protocol.

3.6.6 Post-PCR – SPRI cleaning

The PCR products, which had amplified and were visible as bands on the gel, were cleaned using the SPRI purification protocol. For this method 20 μ L of SPRI beads were added to 20 μ L of PCR products; the DNA to SPRI beads ratio was always 1:1. Thus, the DNA volume was determined prior to adding the beads to ensure the correct amount of each component was used. Pipetting was used to homogenize the mixture, which was left to incubate at room temperature for 5 mins. The PCR tubes with the bead-product mixture were placed on a magnetic plate that caused the DNA-bound magnetic beads to adhere to the sides of the tubes. The remaining liquid (40 μ L) was pipetted away, without removing the beads, and 100 μ L of 80 % ethanol was added to each sample; mixing occurred by pipetting. The alcohol was aspirated without removing the beads. Subsequently, 20 μ L Tris (10 mM, pH 8.0) was added to re-suspend the beads and after 5 mins of incubation at room temperature, the tubes were placed once again on the magnetic plate. The liquid, now containing the DNA, was transferred into new tubes and beads were discarded.

Another 1 % agarose gel was prepared and 1 to 3 μ L of the DNA ladder and stained DNA samples were run at 210 V for 10 mins, to check that the DNA was not lost during cleaning.

3.6.7 Sanger sequencing preparation

For each sample, two times 7.5 μ L of the clean DNA were added to individual 1.5 mL Eppendorf tubes with the addition of 2.5 μ L of the forward primer into one tube and the other receiving the reverse primer used during the PCR. Tubes were each given a barcode sticker (with a unique number) and sent off to Germany (GATC Biotech LightRun) for Sanger Sequencing.

3.7 Sanger sequence data processing

3.7.1 Cleaning of Sanger sequences

Individual sequences were labelled appropriately to indicate whether they belonged to the forward or reverse primer. *FinchTV V 1.5* (Geospiza Inc.) was used to clean the sequences by deleting the bad and weak quality readings of nucleotides and to ensure that primers had been removed.

In *Geneious V 11.0.4* (Biomatters Ltd., New Zealand) one of the sequences to be aligned was reverse complemented and subsequently, two complementary sequences were pairwise multiple aligned. The newly aligned sequence was exported as a consensus sequence and run through *NCBI BLAST/GenBank* to get an indication on what genus or species this sequence might belong to. The five first closest sequences for each sequence were downloaded from *NCBI BLAST/GenBank*, as references for phylogenetics; a note of the accession numbers was made (Table A4).

For nematodes, the selected in-group was *Halomonhystera* spp. based on *NCBI BLAST/GenBank* hits and literature (see Derycke et al. 2007a), and the out-group was *Diplolaimelloides dievengatensis* (based on Tchesunov et al. 2015).

3.7.2 Construction of phylogenetic trees

The free software *MEGA7* (Kumar et al. 2016) was utilized to construct phylogenetic trees. All cleaned Sanger sequenced 18S rDNA nematode sequences (606 bp), downloaded and consensus sequences, were imported into *MEGA7*, and a multiple sequence alignment was created in *MUSCLE* (Edgar 2004). The aligned sequences were screened and identical sequences were deleted apart from one representative sequence. Out of 103 sequences, 21 representative sequences were included in the construction of phylogenetic trees.

After model testing in *MEGA7*, a Kimura 2-parameter model with gamma distribution (K2 + G) (Kimura 1980) was used to build two different types of phylogenetic trees (Maximum-Likelihood (ML) and Maximum-Parsimony (MP) to evaluate the robustness of the alignment. All trees were built with 1000 bootstrap replicates and partial-deletion rates among sites, based on the presence of small gaps among bases. Complete deletion would have disregarded any gaps that might have meaning.

The ML phylogram was edited using *Inkscape V 0.92.4* (Hurst et al. 2019) and MPbootstrap values were added.

No phylogenetic trees for ice polychaete juveniles were constructed due to the lack of sufficient sequences with 500 to 700 bp. Most sequences were around 200 to 250 bp long, which is too short to construct robust phylogenetic trees.

4. Results

4.1 Environmental parameters

4.1.1 Snow depth, ice thickness, and freeboard

The average snow depth at each station varied within two groups: sampling points of low snow cover (between 2 and 6 cm) and those of medium snow cover (between 12 and 19 cm) (Table 1). At station vMF/Mn, snow cover increased from early March (2.2 ± 0.4 cm) to May ($19.2 \text{ cm} \pm 2.7$).

Average ice thickness at each sampling event and site varied between 18.4 ± 0.5 cm and 59.0 ± 0.9 cm throughout the entire sampling campaign (Table 1). The ice was thinnest beginning of March and thickest at the end of April at station vMF/Ref with nearly 60 cm. The ice became thicker throughout the season and grew by 20 cm from March to May at station vMF/Mn (Figure 6).

Table 1. Number of samples/cores for environmental variables for sea ice during the fieldwork in Van Mijenfjorden, in 2017 and 2018. SM= Sympagic meiofauna; Chl *a*= Chlorophyll *a*; ND=No data.

Date [YYYY-MM-DD]	Station	Latitude [Decimal degrees]	Longitude [Decimal degrees]	No. of cores taken				Mean ± StnDev [cm]			Water depth [m]	20 µm net sample depth [m]
				Chl <i>a</i>	SM	Temperature	Salinity	Snow depth [cm]	Ice thickness [cm]	Freeboard [cm]		
2017-03-02	vMF/Ref	77.88453	16.73050	3	3	1	1	18.5 ± 0.5	18.4 ± 0.5	2.7 ± 1.4	2	ND
2017-03-03	vMF/Mn	77.86147	16.71733	3	3	1	1	2.2 ± 0.4	33.1 ± 0.6	2.5 ± 0.5	54	45
2017-03-08	vMF/Mn	77.85058	16.70619	3	3	3	2	12.0 ± 2.6	30.1 ± 0.5	0.6 ± 0.5	54	ND
2017-04-06	vMF/Mn	77.85058	16.70619	3	3	1	1	17.6 ± 5.0	44.3 ± 2.6	3.8 ± 3.0	54	ND
2017-04-07	vMF 1	77.83135	16.61947	3	3	1	1	7.2 ± 0.9	42.3 ± 0.5	1.1 ± 0.6	78	70
2017-04-07	vMF/IM	77.86545	16.70532	3	3	1	1	18.6 ± 0.8	39.0 ± 1.2	1.5 ± 0.0	14	ND
2017-04-23	vMF/Mn	77.86002	16.70693	3	4	1	1	12.7 ± 6.2	51.7 ± 1.6	1.8 ± 1.7	54	50
2017-04-26	vMF 2	77.82590	16.30293	3	4	1	1	6.3 ± 0.8	39.9 ± 0.6	1.6 ± 0.7	61	50
2017-04-27	vMF/IM	77.86038	16.70560	3	4	1	1	18.7 ± 1.9	41.9 ± 1.1	-1.5 ± 0.3	14	ND
2017-04-27	vMF/Ref	77.88453	16.73050	3	3	1	1	13.7 ± 2.5	59.0 ± 0.9	0.5 ± 0.8	2	ND
2017-04-29	vMF/Mn	77.85025	16.70708	3	3	1	1	12.9 ± 2.3	53.8 ± 1.3	1.6 ± 0.7	54	ND
2017-04-30	vMF 1	77.82733	16.61335	3	3	1	1	6.2 ± 1.7	49.4 ± 0.7	2.4 ± 0.7	78	ND
2017-05-02	vMF/Mn	77.86020	16.70985	3	3	1	1	19.2 ± 2.7	53.5 ± 0.7	-1.5 ± 1.4	54	ND
2018-03-24	vMF/Ref	77.88453	16.73050	3	1	1	1	2.0 ± 0.9	67.3 ± 0.6	5.4 ± 0.8	2	ND
2018-03-24	vMF/Mn	77.86147	16.71733	/	Qualitative	/	/	ND	ND	ND	54	ND
2018-04-28	vMF30	77.86325	16.73212	3	Qualitative	1	1	4.6 ± 1.4	92.7 ± 0.8	7.4 ± 1.2	30	ND

The ice thickness and snow depth data along the transect of five stations taken between 26 to 30 April (Figure 7) showed thinnest ice and snow thickness at station vMF2, with 40.0 and 5.5 cm, respectively. Station vMF/Ref had the thickest ice with 59.0 cm and station vMF/IM the highest snow cover with 16.8 cm at the end of April.

Throughout the season, freeboard was variable between stations. Positive freeboard was observed at the start of the spring in March and early April. Negative freeboard was recorded only at one of the transect stations (vMF/IM) in late April and at the start of May (Table 1).

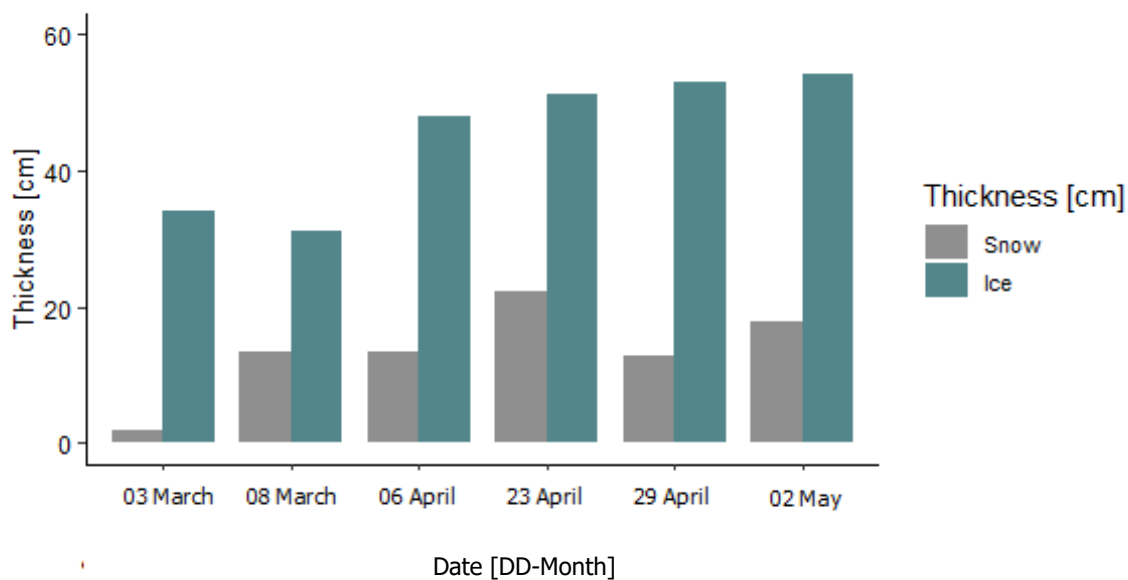


Figure 6. Mean snow depth and ice thickness from station vMF/Mn throughout spring 2017.

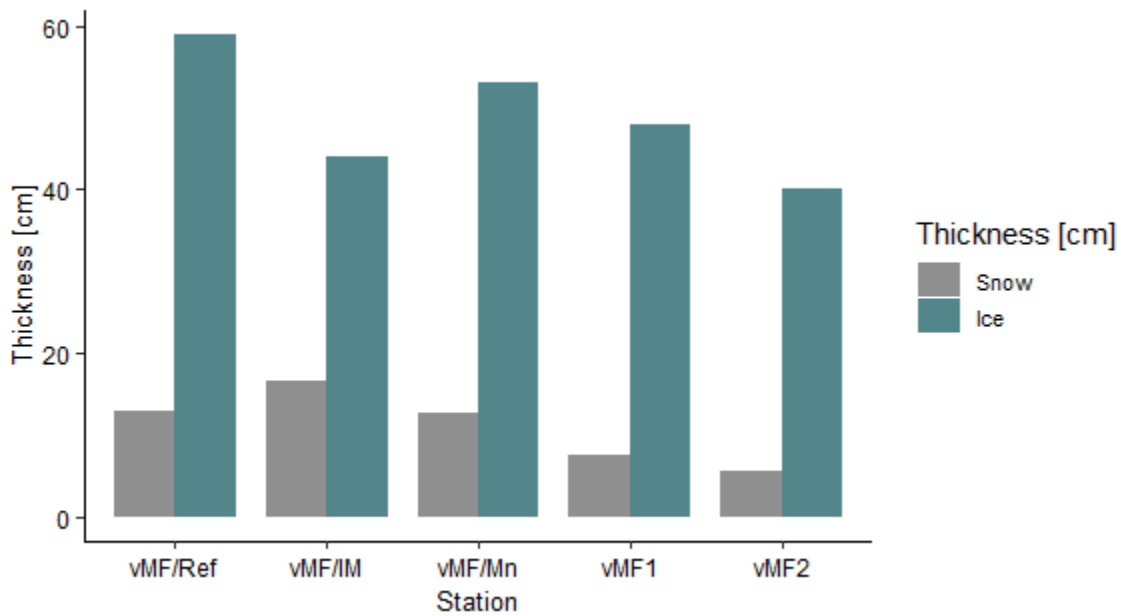


Figure 7. Mean snow depth and ice thickness at the transect stations (26 to 30 April), in Van Mijenfjorden.

4.1.2 Sea ice physics

At the end of April, sea ice temperatures along the transect in Van Mijenfjorden ranged from -5.9 to -1.1°C with coldest temperatures in the top and warmest in the bottom (ice-water interface) of the fast ice. Consequently, the calculated brine salinity was lowest at the ice-water interface with approximately 23 to 40 and higher at the ice-air interface with 23 to 98.

The seasonal changes in sea ice temperature and brine salinity can be observed at station vMF/Mn (Figure 8). The coldest ice temperatures were recorded on 03 March with some fluctuations and warming at the ice-water interface throughout the season. The warmest temperature recorded in the lowermost three centimeters of the ice was -1.4°C at the start of April (06 April). The calculated brine salinity was highest near the ice-air interface and decreased towards the ice-water interface. The lowest brine salinity was recorded on 06 April with 25.2 (Figure 8c).

The transect stations (26 to 30 April), station vMF/IM had the warmest ice temperature both at the ice-air and ice-water interface with values close to -1°C (Figure 9b). Stations vMF/Mn and vMF1 had similar ice temperatures and brine salinities throughout the whole core, whereas station vMF2 has the coldest values out of all stations (Figure 9a).

At the main station (vMF/Mn), the bulk salinity ranged from 8.1 to 22.0 at the ice-air interface and 10.6 to 18.2 at the ice-water interface (Figure B1a). For all dates, bar 08 March and 02 May, the bulk salinity was lowest in the middle section of the ice core. On the other dates, the bulk salinity increased towards the ice-water interface. Bulk salinity among the transect stations (26 to 30 April) ranged from around 3.3 to 18.2 at the ice-air interface and 10.1 to 17.0 at the ice-water interface (Figure B1b). Generally, the bulk salinity increased towards the ice-water interface and was relatively fresh at the ice-air interface.

For all stations, the calculated brine volume was smallest at the ice-air interface and increased towards the ice-water interface (Figure 10). For the main station (vMF/Mn), the brine fraction ranged from 7.8 to 18.3 % at the ice-air interface and 28.0 to 53.2 % at the ice-water interface. For the transect stations, the maximum brine volume was recorded at station vMF/Mn with 53.17 % in the lower one centimeter of the core. At the other stations, it ranged from 28.1 to 52.7 % (Figure 10b).

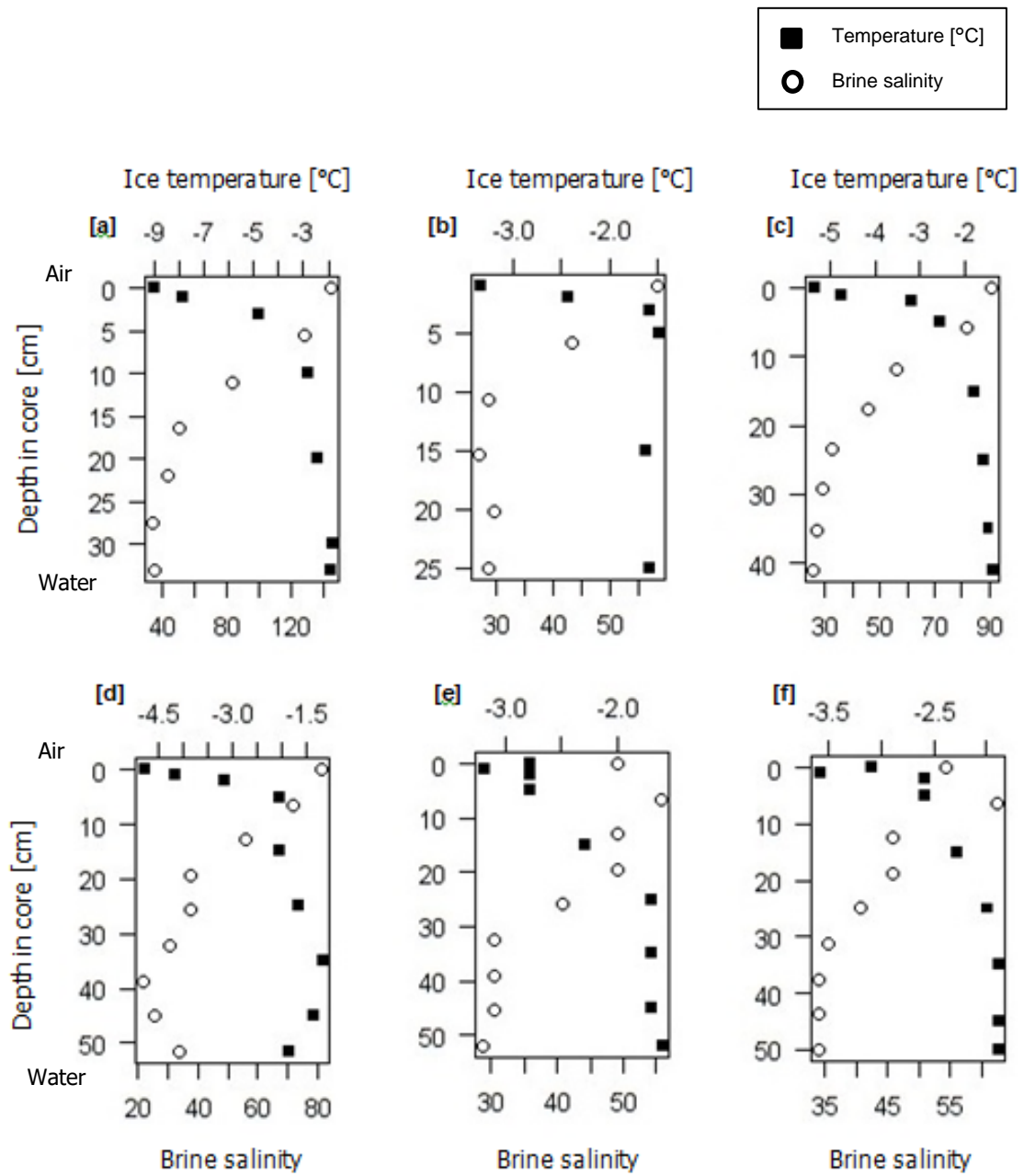


Figure 8. Ice temperature (°C) and brine salinity throughout the season at station vMF/Mn ([a] 03 March; [b] 08 March; [c] 06 April; [d] 23 April; [e] 29 April; [f] 02 May).

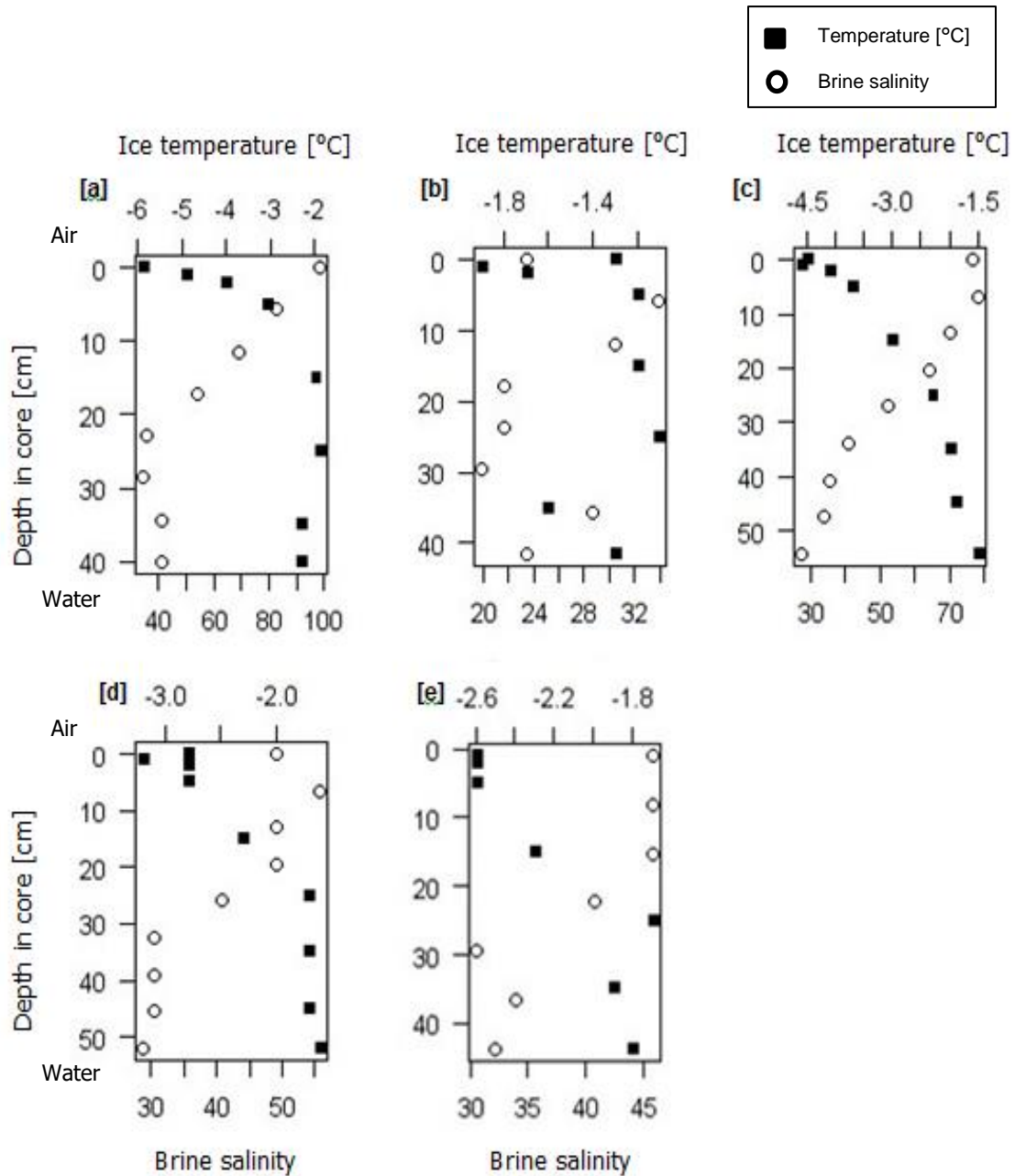


Figure 9. Ice temperature ($^{\circ}\text{C}$) and brine salinity at the transect station (26 to 30 April) in Van Mijenfjorden. ([a] 26 April [vMF2]; [b] 27 April [vMF/IM]; [c] 27 April [vMF/Ref]; [d] 29 April [vMF/Mn]; [e] 30 April [vMF1]).

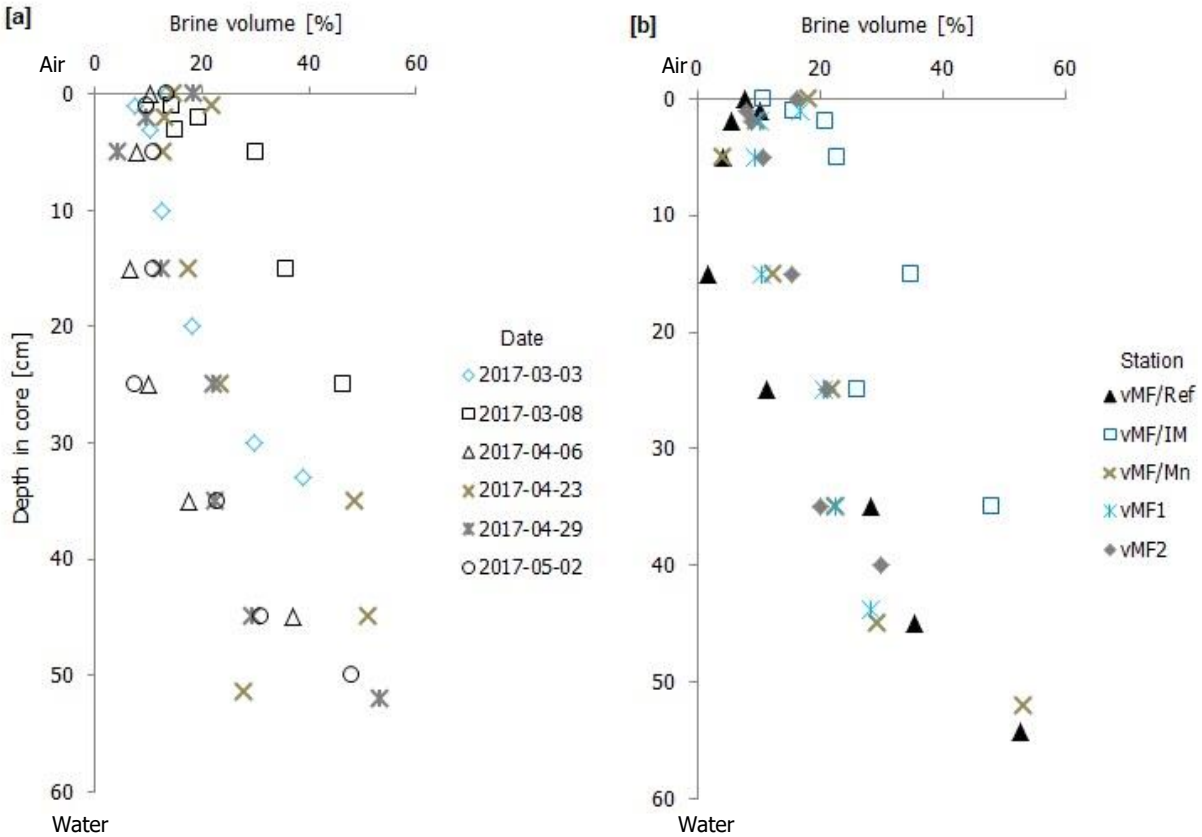


Figure 10. Brine volume (%) calculated for [a] all dates at station vMF/Mn and [b] all transect stations (26 to 30 April).

4.2 Chlorophyll *a* concentration – ice and water

At all stations, the chlorophyll *a* concentration was higher in the ice than in the water by a multiplication factor of 73, at the start of April, which decreased to 35, at the start of May. Water chlorophyll *a* concentrations peaked at the start of May at station vMF/Mn (Figure 11a), which was after the ice algal peak (Figure 11b).

At station vMF/Mn, the ice algal pigment concentration was very low at the start of March ($0.01 \text{ mg chl } a \text{ m}^{-2}$) and increased rapidly towards the end of April when it peaked with $14.74 \text{ mg chl } a \text{ m}^{-2}$ in the lowermost three centimeters of the ice (Figure 12). Beginning of May, concentrations dropped to $4.72 \text{ mg chl } a \text{ m}^{-2}$.

At the transect stations (26 to 30 April), ice algal biomass ranged from 1.37 to $11.46 \text{ mg chl } a \text{ m}^{-2}$, in the three lowermost centimeters of the ice (Figure 13). Overall, station vMF2 had the lowest chlorophyll *a* concentrations recorded.

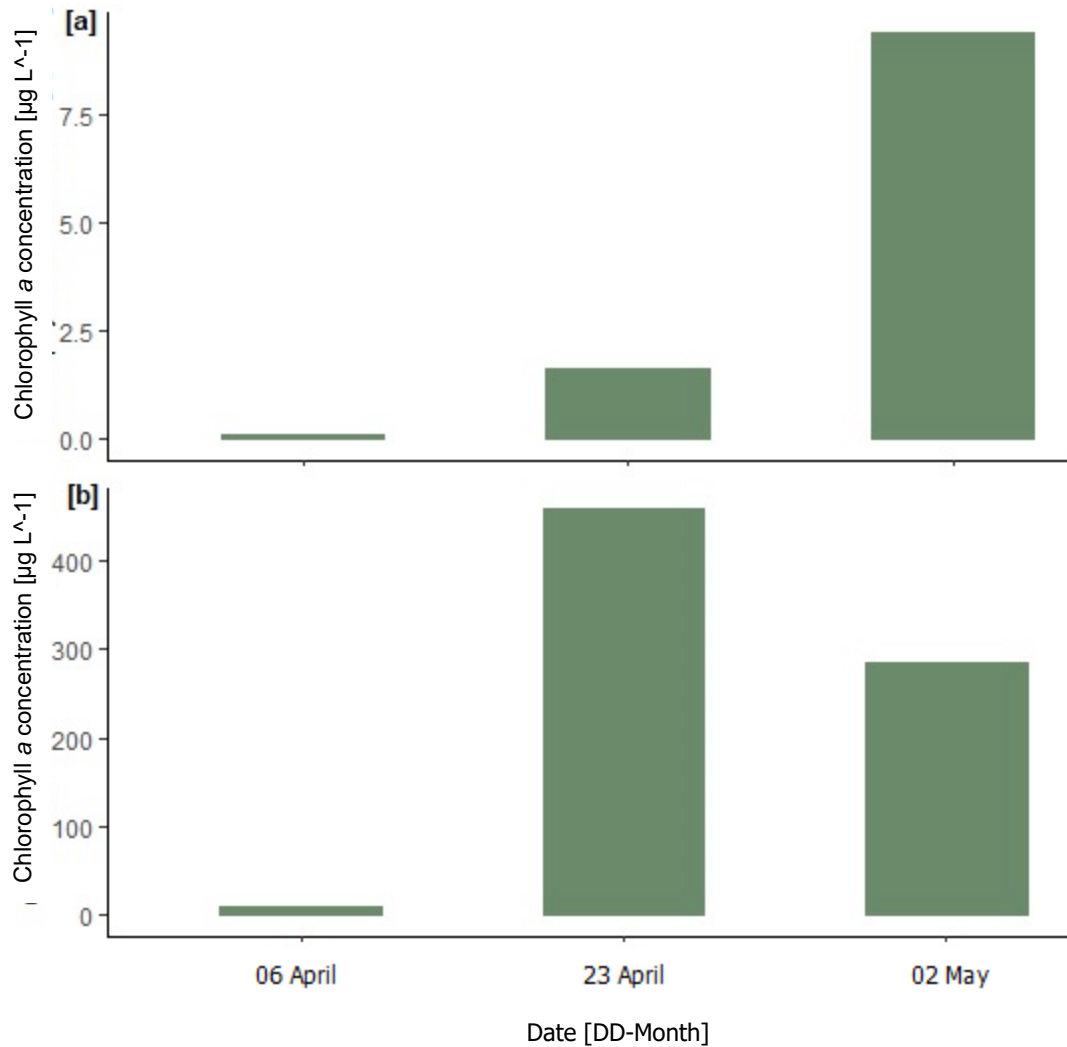


Figure 11. Chlorophyll *a* concentrations in [a] water (0–5 m) and [b] sea ice (0-1 cm), at station vMF/Mn during spring 2017.

At most sampling events, the 3-10 cm ice section contained less chlorophyll *a* than the 0-3 cm section. Only three ice sampling events had the highest algal pigment concentration not directly at the ice-water interface. Two of those samples were collected at station vMF/Mn on 06 April, which had a concentration of 1.67 mg chl *a* m⁻² in the 3-10 cm section compared to 0.24 mg chl *a* m⁻² in the lower three centimeters of the ice (Figure 12). The third sample was collected at station vMF/IM (27 April), which had a higher ice algal biomass in the 3-10 cm section than the 0-3 cm section with 4.64 mg chl *a* m⁻² compared to 3.68 mg chl *a* m⁻² (Figure 13).

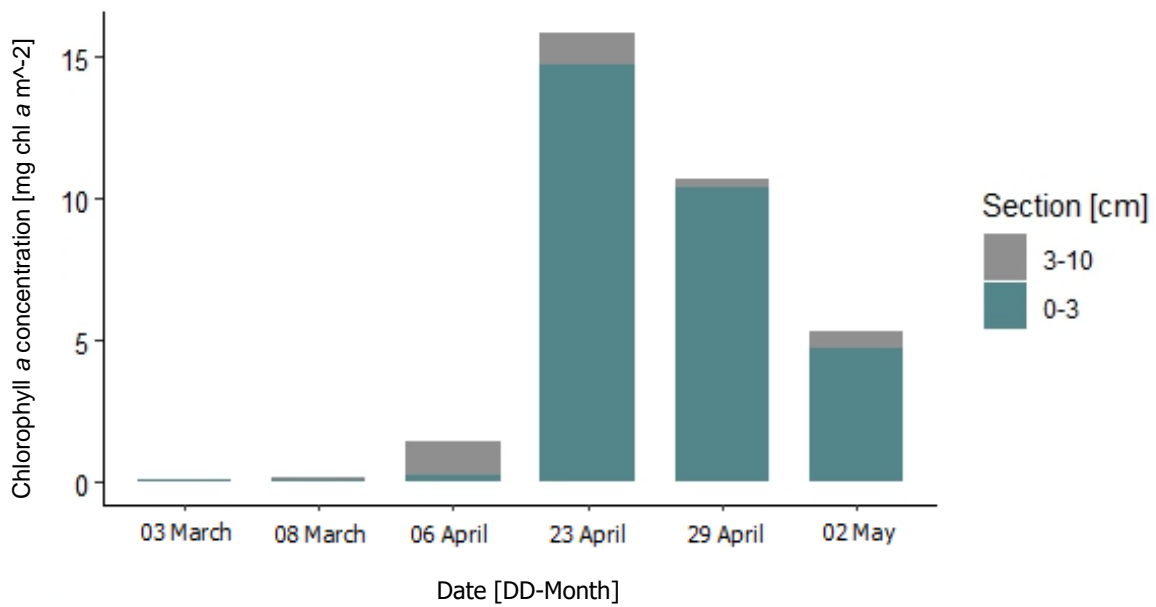


Figure 12 . Integrated chlorophyll *a* concentration (mg chl *a* m⁻²) in the lowermost 10 cm of the ice at station vMF/Mn.

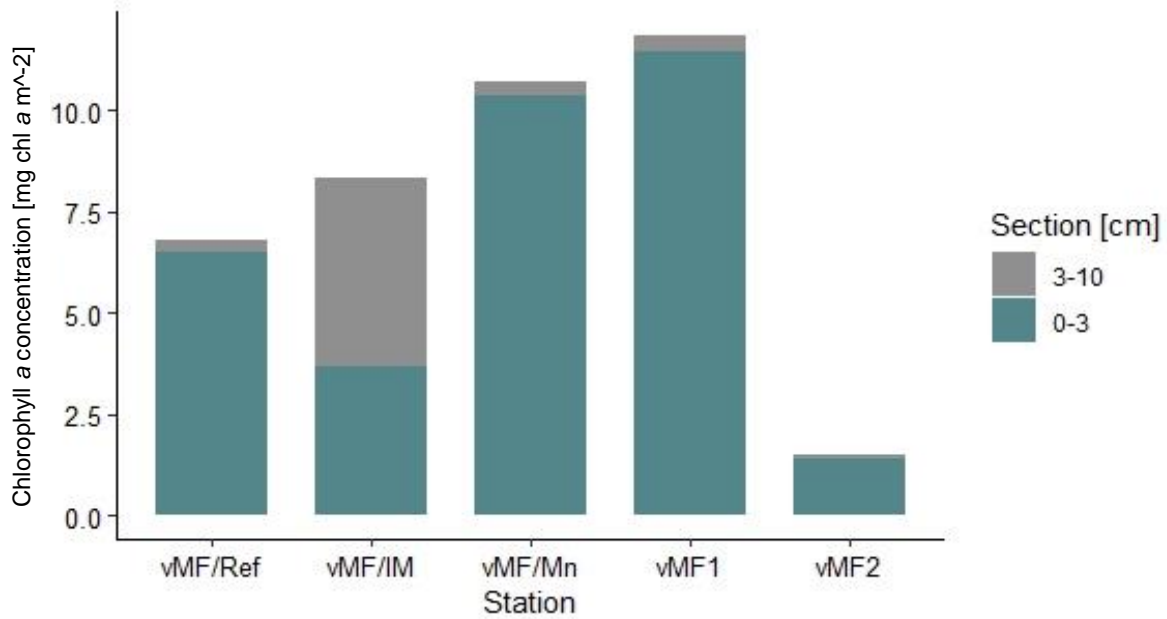


Figure 13. Integrated chlorophyll *a* concentration (mg chl *a* m⁻²) in the lowermost 10 cm of the ice at the transect stations (26 to 30 April).

4.3 Sympagic meiofauna

Highest sympagic meiofauna abundances were located in the lowermost three centimeters of the ice, with absolute highest abundances in the 0-1 cm section. In total, 13 taxa were identified including eggs and unidentified organisms.

4.3.1 Temporal difference

At the main station (vMF/Mn) peak abundances were recorded on 29 April with a total average metazoan abundance of 25,345 ind m⁻² in the lowermost three centimeters of the core (Figure 14a).

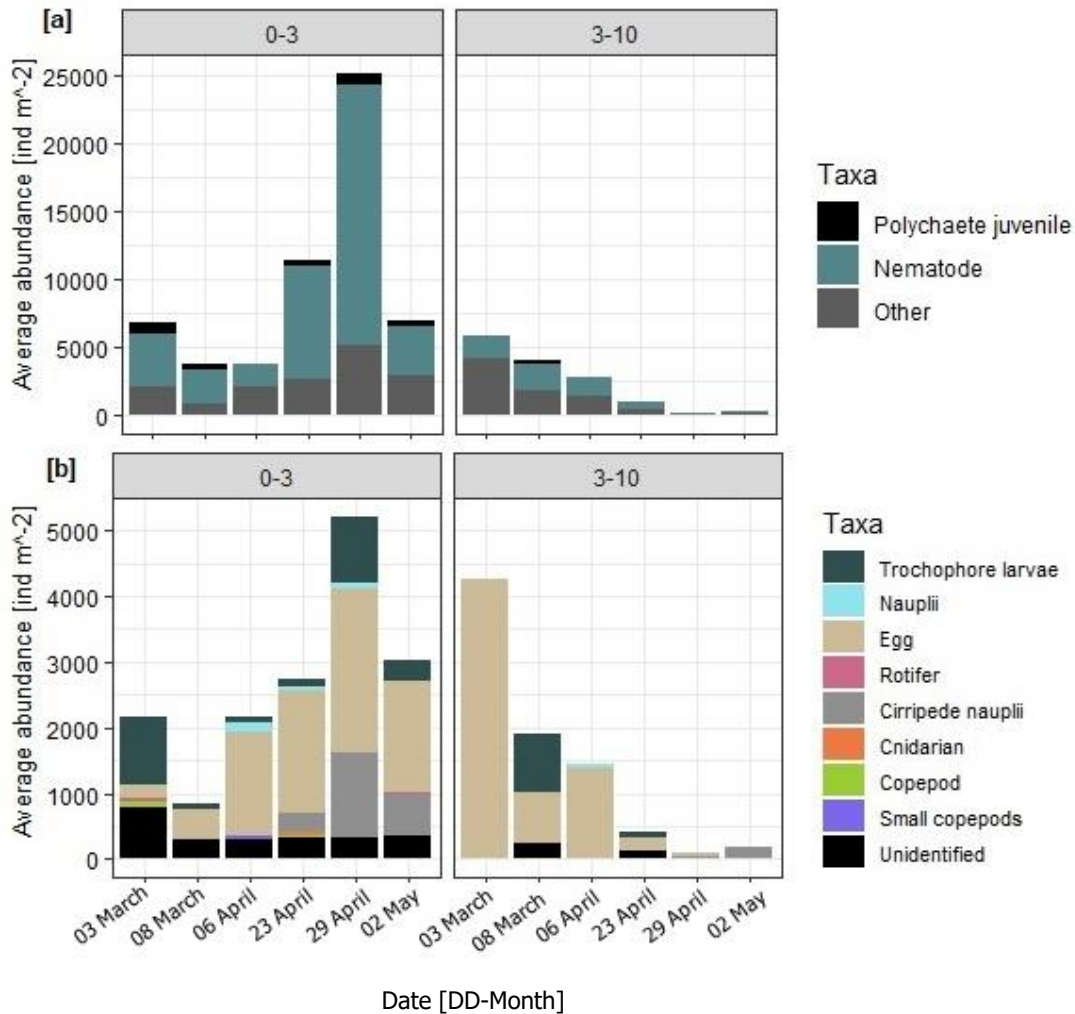


Figure 14. Integrated sympagic meiofauna abundances of [a] the three most abundant fractions and [b] the remaining taxa within the lowermost 10 cm of the ice in two segments at station vMF/Mn.

The lowest total average abundances were observed on 08 March and 06 April with 3,851 and 3,857 ind m⁻², respectively, at the ice-water interface. On all sampling dates at station vMF/Mn, except for 08 March, mean meiofauna abundances were higher in the 0-3 cm section compared to the 3-10 cm section (Figure 14a). Nematodes were the most abundant sympagic meiofauna taxa at the main station, especially in late April. Their abundance increased from the start of March to the end of April from 3,795 to 19,152 ind m⁻² in the three lowermost centimeters of the ice. Seasonal increases in abundances were observed for cirripede nauplii (153 to 1,132 ind m⁻²) and the unidentified fraction (77 to 232 ind m⁻²). Eggs of varying sizes, shape and colour were present at all times with a peak abundance of 4,270 eggs m⁻² at the start of March, which decreased throughout the season, in the 3-10 cm section (Figure 14b).

4.3.2 Spatial difference

Along the ice transect (26 to 30 April), the lowest abundance was found at station vMF2 with 1,556 ind m⁻², which was more than 16 times less than the peak abundance at station vMF/Mn with 25,344 ind m⁻² (Figure 15a). Additionally, diversity was low at station vMF2 with only five occurring taxa compared to station vMF/IM, which had the most diverse sympagic community with nine taxa (Figure 15b).

The highest number of polychaete juveniles was found at the shallow sampling stations vMF/Ref and vMF/IM with 7,554 and 8,860 ind m⁻², respectively, in the lowermost three centimeters of the ice (Figure 15a). At station vMF/Mn, only 810 polychaete juveniles m⁻² were present in the 0-3 cm section; no juvenile polychaetes were found at stations vMF1 and vMF2.

The 'other' fraction at all stations, apart from station vMF/Ref, was dominated by eggs. At the innermost station (vMF/Ref), rotifers were more abundant than eggs with 766 ind m⁻² compared to 51 eggs m⁻² (Figure 15b).

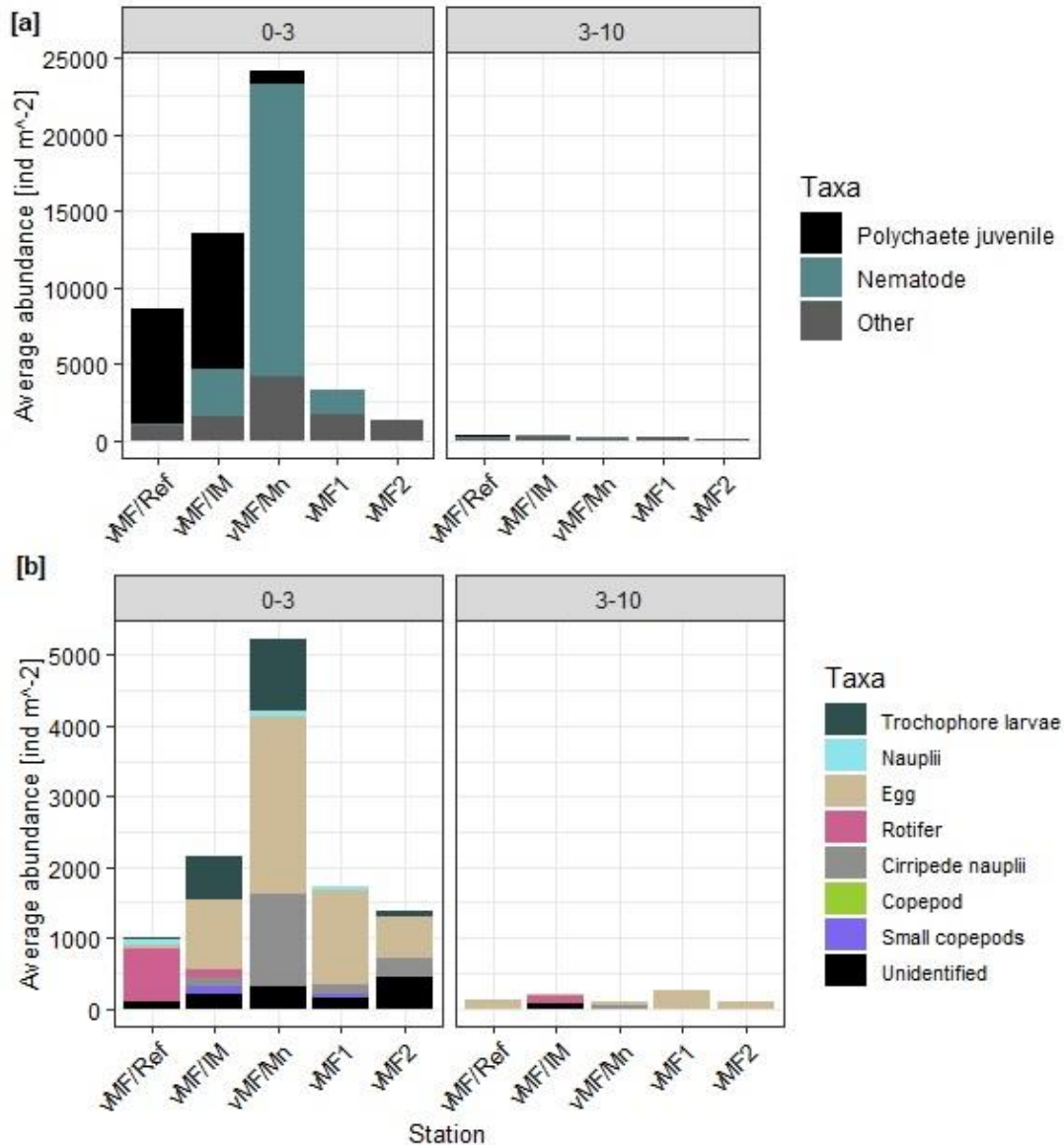


Figure 15. Integrated sympagic meiofauna abundances of [a] the three most abundant fractions and [b] the remaining taxa within the lowermost 10 cm of the ice in two segments at the transect stations (26 to 30 April).

4.3.3 Sympagic meiofauna-environmental correlations

A Spearman's rank correlation test was used to assess the correlation between the abundance of nematodes and chlorophyll *a* concentration, in the lower one and three centimeters of the ice. At station vMF/Mn, nematode abundance was not significantly positively correlated to ice algal biomass, either in the lower three centimeters of the ice ($Rho = 0.77$, $p = 0.1$) nor the 0-1 cm section ($Rho = 0.83$, $p = 0.06$).

A significantly positive correlation to chlorophyll *a* was found for total sympagic metazoan abundance at the main station (vMF/Mn) (Rho = 0.88, *p* = 0.03), in the lowermost three centimeters of the ice.

No significant correlations were found between any environmental variable and metazoan abundance (in the lowermost 10 cm of the ice) for the main station (vMF/Mn) or the transect stations (26 to 30 April), apart from juvenile polychaete abundance and water depth (Rho = -0.872, *p* = 0.05) (Table B1). This correlation was further tested in with a Quasi-Poisson regression that resulted in a *p*-value of *p* < 0.001.

4.4 Microzooplankton abundance

The microzooplankton net samples (> 20 µm) yielded slightly higher diversity than the sea ice with 15 taxa present including eggs and unidentified organisms (Table B2). All sympagic taxa were present in the net samples with varying degrees of abundance. The difference in taxa between ice and net samples arose from the presence of *Acartia longiremis*, chaetognaths and cnidarians. Although both the net and ice samples contained cnidarians they were morphologically different (e.g. *Sarsia* sp. in the water and potentially *Sympagohydra tuuli* in the ice).

Polychaete juveniles and nematodes were more abundant in the lowermost three centimeters of ice than in the water column (Figure 16a). At station vMF/Mn in early March, only 108 nematodes m⁻² were found in the water compared to 3,795 nematodes m⁻² in the ice. As the season progressed the number of nematodes in the water column did not increase, whereas the number of sympagic nematodes did. The reverse occurred for polychaete juveniles. Their abundance in the ice decreased at station vMF/Mn from 956 (03 March) to 377 ind m⁻² (23 April), whereas it increased in the water from 0 to 154 ind m⁻² (Figure 16b). Nevertheless, polychaete juveniles were still more abundant in the ice than the water column. Additionally, net samples from station vMF/Mn had a lower number of eggs than the ice samples from the same dates.

Microzooplankton samples from station vMF2 (26 April) exhibited low abundance or absence of polychaete juveniles and nematodes. Other faunal taxa such as small copepods and cirripede nauplii dominated the net samples at all stations (Table B2).

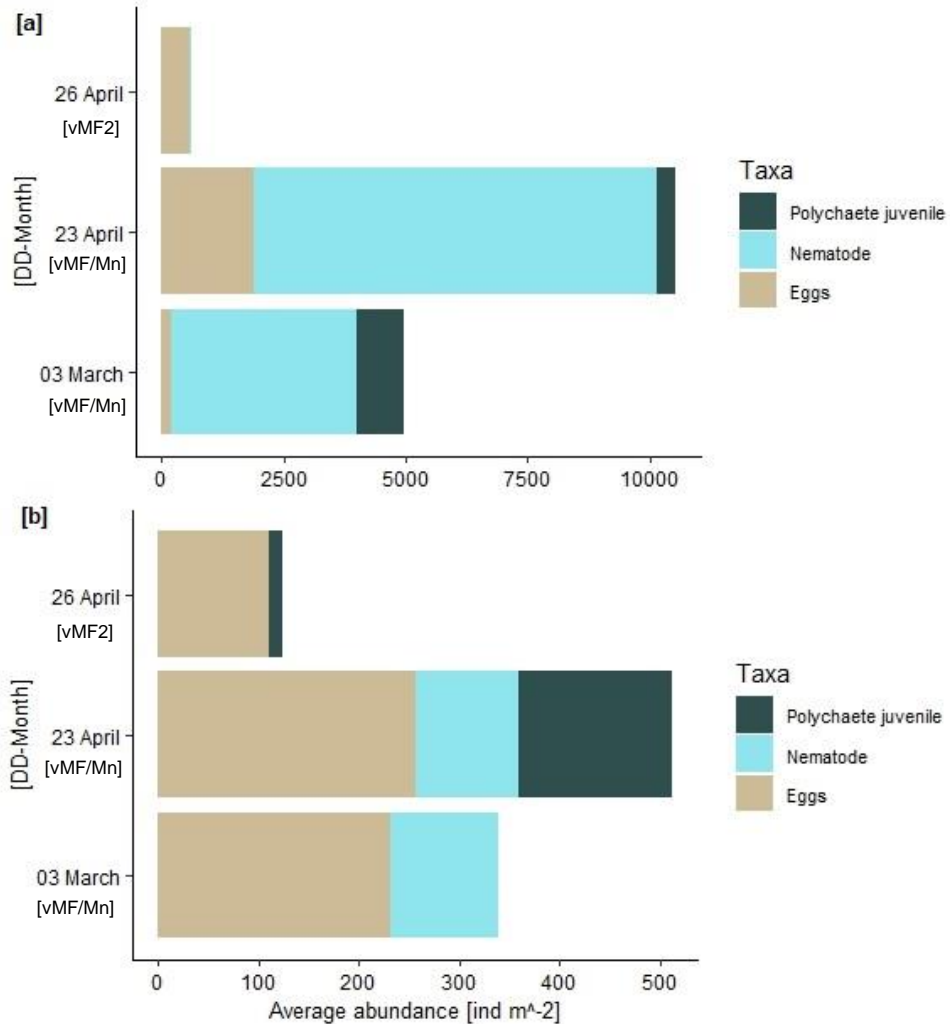


Figure 16. Average abundance of the three target organisms in the [a] sea ice (0-3 cm) and [b] entire water column (at stations vMF/Mn and vMF2) throughout spring 2017.

4.5 Size of sea ice nematodes and polychaetes collected from the ice and during experiments

4.5.1 Nematodes

A total of 132 nematodes were measured mainly at station vMF/Mn where they were most abundant. Nematodes ranged in body length from 175 to 3,234 μm with a decrease in length as the season progressed (Figure 17a).

At the start of March, 92 % of the individuals fell within the adult size class ($> 1700 \mu\text{m}$). By the end of April, smaller juvenile nematodes started to appear and 49 % of the measured

nematodes were $< 1700 \mu\text{m}$ in length by the start of May (Figure 17b). The majority of juvenile nematodes were situated in the 0-3 cm section of the ice cores.

4.5.2 *Polychaete juveniles*

A total of 70 polychaete juveniles were measured at various stations, over a period of 61 days, in spring 2017. They ranged in size from 250 to 2,119 μm with an increase in length towards the end of the season in May (Figure B2a).

Comparatively, juvenile polychaetes (collected in late March 2018) were on average between 501 to 533 μm long (at the start of the experiment) and grew to a maximum size of 1,117 μm , in the high food treatment, over a period of 44 days (Figure B2b).

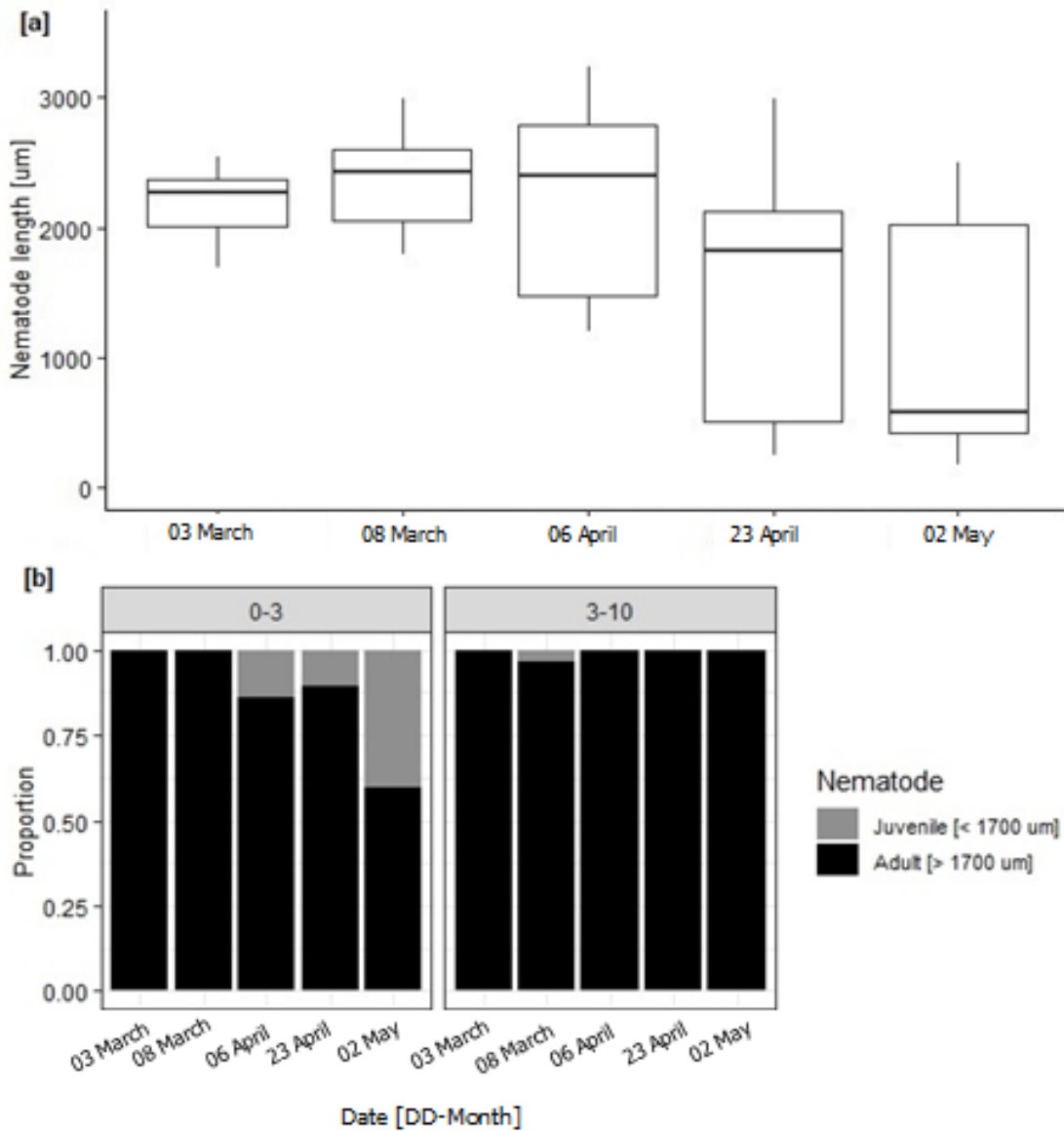


Figure 17. [a] *in situ* sympagic nematode length (µm) and [b] proportion of juvenile to adult nematodes in sea ice samples at station vMF/Mn, throughout spring 2017.

4.6 Polychaete growth experiment

The initial mean number of setiger ranged from 3.3 ± 0.4 to 3.9 ± 0.4 compared to 5.1 ± 0.9 to 9.6 ± 3.0 by the end of the experiment (Table 2). In the first three weeks of the experiment, the number of setiger did not differ between the different food treatments (Figure 18). After 23 days, the medium and high food treatment started to diverge from the control and low treatment, as the mean setiger number started to increase.

Mortality rates ranged from 30 to 56 % in all treatments with the lowest survival rate in the control and low food treatment; loss of segments was observed in some treatments.

Table 2. Mean number of setiger (\pm StnDev) at the start and end of the polychaete juvenile growth experiment.

Treatment	Control	Low	Medium	High
Start	3.9 \pm 0.4	3.5 \pm 0.6	3.5 \pm 0.6	3.3 \pm 0.4
End	5.1 \pm 0.9	5.9 \pm 0.9	7.6 \pm 1.4	9.6 \pm 3.0

There was a significant difference in polychaete larvae development between food treatments for the medium (GAMM, $p = 0.00148$) and high ($p < 0.001$) compared to the control treatment, but not between the control and low treatment ($p = 0.470$) (Figure B3). Additionally, morphological features developed more distinctly in the medium and high treatment than in the low and control treatment (Figure 19). In the medium and high food concentration, all polychaete juveniles developed long, obvious palps, whereas in the control and low treatment palp development was reduced. For comparison, at the end of the experiment average palp length in the control and low was 40.2 and 38.5 μm , respectively, while the medium and high food treatment had average palp lengths of 67.9 and 104.6 μm .

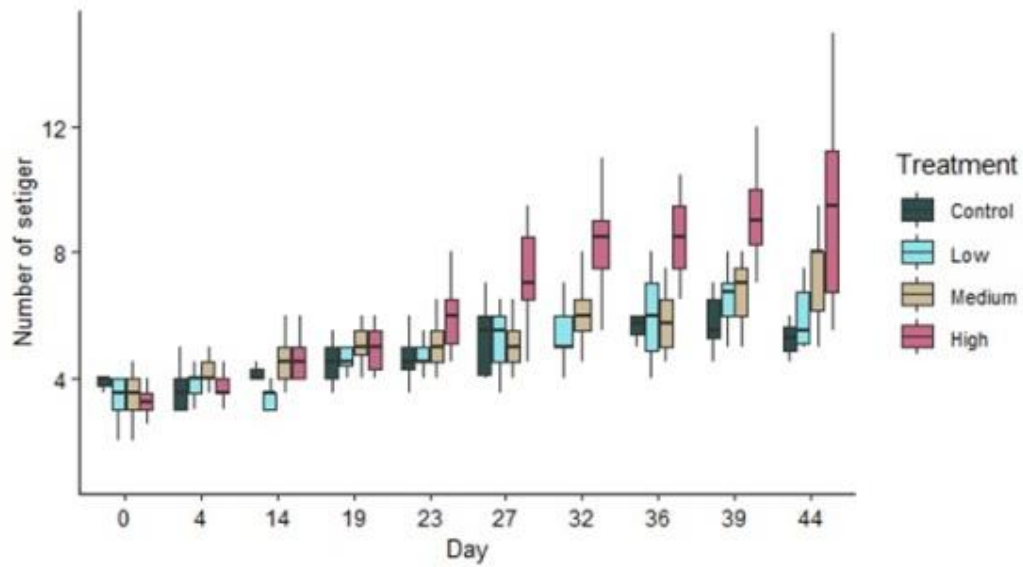


Figure 18. Number of setiger of juvenile polychaetes in each treatment over the duration of the experiment with no outliers. All data are represented by the boxplots.

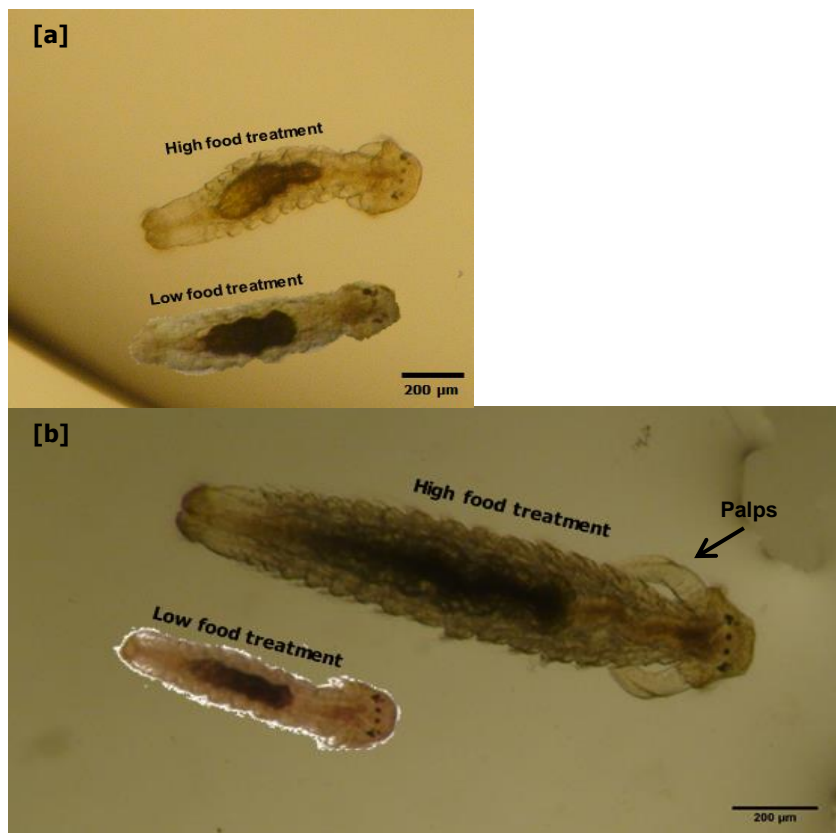


Figure 19. Morphological development of polychaete juveniles in low and high food treatment from [a] day 14 and [b] day 44.

4.7 Molecular data

4.7.1 Nematodes

The sympagic nematode sequences (n=61) from Svalbard formed their own clade (Figure 20). Sequences from Van Mijenfjorden, Palander- and Inglefieldbukta clustered together, but formed a separate clade from the reference sequences (Table A4) with high support (bootstrap values for ML and MP were 99, 99 and 87, 93). They appeared to be most closely related to the reference sequences of *Halomonhystera* sp. (HF572952.2 and MG669808.1) and GD1_H with high support (bootstrap values for ML and MP were 99, 98).

Wahlenbergfjorden formed a different clade and appeared more closely related to the *Theristus* sp. reference sequences than any of the other sequences with high support (bootstrap values for ML and MP were 100, 100).

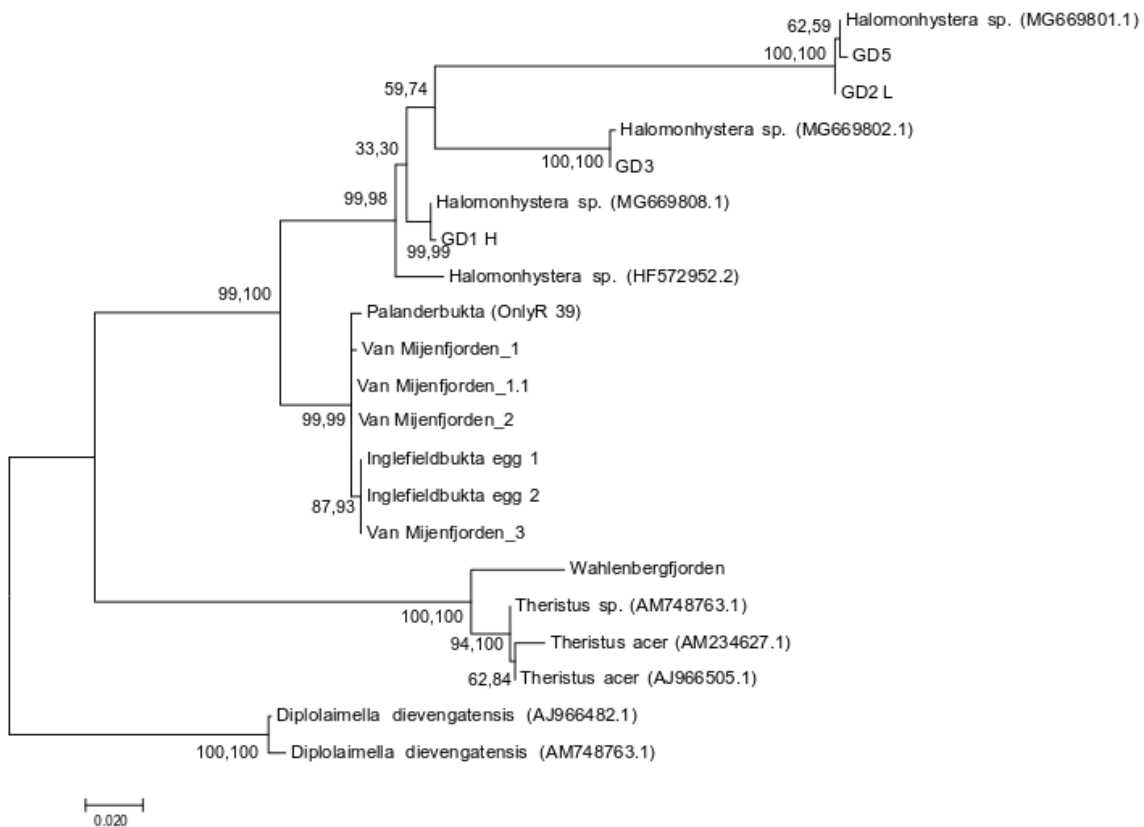


Figure 20. Maximum-likelihood tree produced from 61 sympagic nematode 18S rDNA sequences. Bootstrap values correspond to maximum likelihood (ML) and maximum parsimony (MP). *Diplolaimella dievengatensis* (accession number AJ966482.1 and AM748763.1) served as an outgroup.

The pairwise distance values were in agreement with the phylogenetic tree (Table 3). The Svalbard clade had relatively low divergence (7.1 – 8.3 %) from reference sequences of *Halomonhystera* sp. (HF572952.2 and MG669808.1) and GD1_H. Comparatively, divergence rates were higher for GD2_L and GD5 with 19.8 – 20.2 % and 24.5 – 24.8 %, respectively.

The Wahlenbergfjorden specimen had low divergence from the *Theristus* sp. sequences with 1.0 – 4.6 %, but higher divergence to the *Halomonhystera* sp. (HF572952.2 and MG669808.1) and GD1_H with 22.1 – 23 %.

Table 3. Pairwise distance (%) values for 18S rDNA for sympagic nematodes from Svalbard and reference sequences from intertidal *Halomonhystera* sp. (HF572952.2, MG669808.1 and GD1_H) and *Theristus acer* (AJ966505.1).

VM – Van Mijenfjorden, IB – Inglefieldbukta, PB – Palanderbukta and WB – Wahlenbergfjorden.

	MG669808.1	GD1_H	HF572952.2	VM_1	VM_2	IB_egg	VM_3	PB
MG669808.1								
GD1_H	0.2							
HF572952.2	2.8	2.9						
VM_1	7.1	7.3	8.1					
VM_2	7.0	7.1	7.9	0.2				
IB_egg	7.3	7.5	8.3	0.5	0.3			
VM_3	7.3	7.5	8.3	0.5	0.3	0		
PB	7.3	7.5	8.3	0.5	0.3	0.7	0.7	
WB	22.3	22.1	23.0	20.1	20.3	20.8	20.8	20.3
AJ966505.1	20.1	19.9	21.4	20.1	20.3	20.7	20.7	20.5

4.7.2 Polychaete juveniles

Overall, out of the 15 polychaete juvenile DNA samples sent off, seven sequences revealed a match to Spionidae sp. in the *NCBI/GenBank* database. These sequences had a query cover and ID match of 93 to 99 % (Table B3); any other sequences were disregarded.

5. Discussion

5.1 *Sea ice as a reproductive and nursery ground*

In Arctic landfast ice, sympagic meiofauna communities tend to be dominated by nematodes or by the larval stages of pelagic and benthic organisms. In addition, morphologically different eggs can be found in sea ice throughout the spring (e.g. Marquardt et al. 2011). In Van Mijenfjorden, the sympagic meiofauna community followed a similar pattern to those observed from other studies (e.g. Horner et al. 1992; Bluhm et al. 2018). Additionally, it became apparent that ice nematodes were using the sea ice mainly over deeper water (> 50 m) as a reproductive ground, whereas polychaete juveniles were using the ice as a nursery ground over shallow water (2 – 14 m).

At the start of the season, chlorophyll *a* concentrations and food availability were low at all stations. Low solar angle and irradiance meant that ice algae were not able to grow exponentially yet. Nevertheless, a high abundance of juvenile polychaetes was found at the innermost station (vMF/Ref) (Figure B4) and adult nematodes (> 1700 μm) were already present at the main station (vMF/Mn). Nematodes are known to exploit different food niches, such as dissolved organic matter (DOM), bacteria and/or algae, depending on what the highest quality available food source is (Jensen 1987). Bacterial biomass in sea ice can exceed concentrations in the water column (e.g. Deming and Collins 2017), especially early on in the season after a rather unproductive and dark winter. Tchesunov and Riemann (1995) suggested that sympagic nematodes might be using bacteria as an alternative food source when ice algae are not readily available. Being able to exploit other food sources could explain the lack of a significant positive correlation between ice algal biomass and nematode abundance. Further support for this arises from the lack of gut colouration, in March and early April, opposed to later on in the season when all adult nematodes had green guts. As the season progressed, chlorophyll *a* concentrations started to increase and nematodes appeared to be feeding on ice algae, using the energy gained to sexually mature and to produce eggs. Nematodes with well-developed gonad structures were observed (Figure B5), which was followed by the appearance of nematode eggs. The presence of nematode eggs was confirmed through observations of juveniles moving in the eggs, hatching and molecular tools. The sequences obtained from the nematode eggs clustered together with the sequences from adult nematodes.

An increase in the number of nematodes coincided with the appearance of small juveniles (< 1700 μm), especially on 29 April (station vMF/Mn). Nematodes that belong to the family Monhysteridae (e.g. Riemann and Sime-Ngando 1997; Derycke et al. 2007a) have a high reproductive output. Tchesunov (1986) observed that at the end of April over 95 % of the nematodes in the ice, belonging to this family, were juveniles. The nematodes collected in Van Mijenfjorden are thought to belong to the Monhysteridae family (based on molecular tools) and thus an increase of 10,866 ind m^{-2} in less than one week would not be unsurprising considering their high reproduction potential. Further support for this statement arises from the number of nematode eggs per pouch that were observed *in situ*. Each cluster found in the sea ice contained at least eight eggs. Considering that at the main station (vMF/Mn) egg abundances generally reached over 1,000 ind m^{-2} , in April, an increase of over 10,000 nematodes m^{-2} is feasible. Interestingly, the majority of nematode juveniles hatched after the peak in ice algal biomass at the main station (vMF/Mn), which could be an alternative explanation for the lack of a significantly positive correlation between chlorophyll *a* and nematode abundance. Lee (2002) stated that hatching of juveniles from eggs only occurs under favourable environmental conditions. Although hatching occurred after the chlorophyll *a* maximum, juveniles still hatch when food availability was high and environmental conditions were within tolerable limits of ice nematodes (Friedrich 1997).

Benthic polychaete juveniles appear to be using the sea ice as a nursery ground and refuge, in Van Mijenfjorden. Although ice algal biomass was low at the start of the season, juvenile polychaete abundance was high at station vMF/Ref. The same was observed by Grainger and Hsiao (1990) that found higher abundances of polychaete juveniles in sea ice in March compared to later on in the season. High numbers of juvenile polychaetes, early on in the season, could be explained by sea ice acting as a nursery ground and refuge from predators (e.g. Marquardt et al. 2011). Support for this theory arises from the feeding experiment conducted in this study. Even at low food concentrations, polychaete juveniles grew. Albeit, development was much slower compared to the medium and high food treatment, colonizing sea ice, in early spring, ensures that juvenile polychaetes are present when ice algal biomass increases and at the same time sea ice provides protection from predators. The only carnivorous organism recorded from inside sea ice, *Sympagohydra tuuli* (Bluhm et al. 2007; Marquardt et al. 2018), is rare in Van Mijenfjorden.

Subsequently, it can be assumed that landfast ice is a safe place for juvenile polychaetes in spring. Additionally, McConnell et al. (2012) showed that growth rates of polychaete juveniles were faster in sea ice due to highly concentrated ice algae compared to growth at coherent phytoplankton concentrations. Microalgae biomass was higher in sea ice than the water column until May, in Van Mijenfjorden. Thus, it is advantageous to colonize sea ice from early on in the spring season for growth and development of polychaete juveniles.

When food is not limiting, polychaete larvae are able to grow in body length, become wider and develop distinct morphological features indicative of maturation (e.g. palps). Coincidentally, this development was observed mostly in the medium and high food treatment, and *in situ* towards the start of May when the largest and morphologically most-developed polychaete juveniles were found in sea ice samples, especially at the innermost station (vMF/Ref).

Polychaete juvenile abundance decreased towards the end of April at the shallowest station vMF/Ref, which could be explained by the environmental conditions at this station at the end of April. Polychaetes are known to be negative phototaxis. As the season progresses, melting snow coupled to increasing solar angle and day length, means that more and more light is being transmitted through sea ice. This increase in light might act as an external cue for polychaete juveniles to migrate to the benthos to complete their metamorphosis to adults, causing a decrease in their abundance. Transmittance through the ice increased in Van Mijenfjorden as the season progressed (Kvernvik 2018), meaning that light could have initiated the downward migration and subsequent decrease in polychaete juvenile abundance at the innermost station (vMF/Ref). Furthermore, station vMF/Ref had been colonized since early March, meaning that at the end of April a proportion of the juvenile polychaetes must have been at a stage to complete their metamorphosis in the benthos causing them to leave the ice. Considering the body length (1,022 to 2,119 μm) and distinct palps of observed polychaete juveniles, this seems like a valid assumption. Molecular tools indicated that the juveniles polychaetes found might belong to the family Spionidae, which needs sediment as an adult to build tubes in order to feed (e.g. Dauer 1983).

Although early life stages of pelagic and benthic organisms tend to dominate sympagic meiofaunal communities, another abundant and interesting sympagic fraction across the Arctic is eggs (e.g. Marquardt et al. 2011). Overall, six morphologically different eggs were found in Van

Mijenfjorden. At the main station (vMF/Mn), the number and variety of eggs increased throughout the season, as more food to fuel reproduction, in the form of ice algae, became available. Furthermore, depending on the organism, laying eggs in late spring might ensure a match between the hatching of larvae and the phytoplankton bloom (e.g. Søreide et al. 2010). Even at the transect stations with low sympagic meiofauna abundance (e.g. station vMF2) eggs were abundant. Consequently, not only is sea ice an important reproductive and nursery ground to pelagic and benthic larvae, but it can also harbor a wide-variety of eggs that might either be directly deposited into the ice (e.g. nematodes) to ensure that hatchlings have access to a highly concentrated food source and/or they end up in the ice indirectly (e.g. through scavenging during ice formation), but ultimately are protected from predators in the water column.

5.2 Spatial differences in sympagic meiofauna abundance

The spatial variability of sympagic meiofauna was investigated along a depth transect at the end of April. Water depth is known to be a controlling factor that influences sympagic communities, with depths of > 50 – 70 m favoring pelagic organisms (Gulliksen and Lønne 1991) and shallow waters (< 50 m) leading to meroplankton dominated communities (Gulliksen and Lønne 1991; Bluhm et al. 2018). In this study, this trend was primarily reflected in the juvenile polychaete abundance, which appeared to be controlled by water depth ($p < 0.01$). The absence of ice polychaete juveniles at the deepest stations vMF1 (78 m) and vMF2 (61 m) further confirm this theory, for spring 2017.

Not only did the abundance of ice meiofauna differ between stations, but also the community composition. Due to tighter sympagic-benthic coupling at the shallowest station vMF/Ref (2 m water depth), a higher abundance of benthic fauna, predominately juvenile polychaetes, was found. At the deeper stations, less or no benthic larvae were observed, except for cirripede nauplii at stations vMF/Mn (50 m) and vMF2 (61 m). Cirripede nauplii are known to ‘bloom’ at the end of April/early May in Svalbard fjords (Stübner et al. 2016) and high abundances appear not be limited to shallow waters even though they originate from sessile benthic adults. Nematodes collected from the sea ice in Van Mijenfjorden most likely belong to the family Monhysteridae (based on molecular tools) of which all known marine genera live in the sediment (e.g. Fonseca and Decraemer 2008). Thus, even at the deeper stations (> 50 m), there might be stronger sympagic-benthic than sympagic-pelagic coupling, in Van Mijenfjorden.

The intermediate station (vMF/IM) had the most diverse community with a mixture of pelagic and benthic organisms. This could be linked to the water depth, which is neither too deep nor too shallow (14 m) allowing both pelagic and benthic organisms to colonize the ice. The polychaete juvenile community found at station vMF/IM appeared to be in an earlier development stage compared to the innermost (vMF/Ref) station. This speculation arises from the smaller sized polychaete juveniles found at the intermediate station (vMF/IM) compared to the ones at station vMF/Ref.

Several environmental parameters could have caused the low faunal abundance at stations vMF1 and vMF2. Ice algal biomass and thus food availability for herbivorous sympagic meiofauna was very low at station vMF2. At the end of April, warm water was detected in the fjord (pers. comm. Eva Leu), which would have reached station vMF2 first and lead to ablation of ice algal biomass. Furthermore, ice algae require nitrate (NO_3) in order to photosynthesis and grow (Eberhard et al. 2008). Kvernvik (2018) found that NO_3 levels in Van Mijenfjorden were low under low snow cover, of which the latter was the case at station vMF2. Therefore, this station might have been representative of advanced post-bloom conditions, where most ice algae had left the ice sheet leaving insufficient food for the maintenance of a sympagic meiofaunal community. This assumption appears reasonable considering that the brine salinity and *in situ* ice temperature were within the tolerable limits of sympagic meiofauna (e.g. Grainger and Mohammed 1990; Friedrich 1997). Alternatively, the sea ice at station vMF2 was the youngest sampled in 2017. Due to its young age, but late formation in the season, environmental conditions for the establishment of sympagic flora and fauna communities might not have been favorable anymore. Considering the low snow cover, but high solar angle and day length, this station must have been an unfavorable place to colonize and inhabit.

Interestingly, station vMF1 had low sympagic meiofauna abundance despite high food availability and favorable environmental conditions. The snow cover at station vMF1 was low throughout spring, which leads to increased light transmittance through ice. Although this might initially benefit ice algae, as they receive sufficient photosynthetic active radiation (PAR) grow exponentially. However, Leu et al. (2010) have shown that prolonged exposure to high irradiance due to low snow cover can lead to a decrease in ice algal food quality without affecting growth. Therefore, it could be assumed that despite high chlorophyll *a* concentrations in the sea ice at

station vMF1, the quality of the available food was poor and thus little sympagic meiofauna colonized the ice.

Differences in community composition between stations could arise not only from the different bottom depths, but also from the type of sediment on the seafloor. Renaud et al. (2007) found that the benthic community composition in Van Mijenfjorden varied between the inner, mid and outer basin due to structural differences on the seafloor (e.g. sediment type). In autumn 2018, the sediment sample retrieved from the innermost station (vMF/Ref) was dominated by sandy sediment of larger grain size and higher water content than the sediment at the deeper stations (vMF/Mn, vMF1 and vMF2). At those stations, the sediment consisted of clay-like material with little water content and high compaction. Station vMF/Ref was characterized by sediment that is known to be favored by Spionidae sp. (e.g. Dauer 1983; Souza and Borzone 2000). The larger grain size of the sand allows adult polychaetes to effectively bury themselves and build tubes (from sand and mucus) from which their palps can extend to capture particles at the sediment-water interface (Dauer 1983; Souza and Borzone 2000; Spreybroeck et al. 2007). The clay-like material at the deeper stations might be too tightly packed for the family of polychaete juveniles (potentially Spionidae) found in the sea ice in Van Mijenfjorden. Although the largest individual grown in the laboratory was less than 3,000 μm , juvenile polychaetes observed were wider than nematodes. This could imply that the sympagic polychaete juveniles found were simply too big for the tightly packed sand grains, at the deeper stations. Furthermore, the shallowest station (vMF/Ref) is most influenced by the tides every day. Polychaetes within the Spionidae family are most commonly found in waters with high current speeds, as they trap food particles from the ambient water with their palps (Dauer 1983). As their palps lack food grooves, they need to inhabit a high energy environment in order to efficiently feed (Dauer 1983). Therefore, the conditions at the innermost station are most favorable with daily water exchange that not only ensures good water flow, but also replenishment of nutrients that encourages microalgal growth (pers. comm. Eva Leu), making food readily available.

Szymelfenig et al. (1995) showed that nematode abundances tended to peak in muddy-sand in Van Mijenfjorden, which is in accordance with Heip et al. (1985) that found that with decreasing sediment grain size, nematode abundance increased. Therefore, there could be a correlation between high abundances of nematodes at the deeper stations (e.g. vMF/Mn – 50 m) and the presence of fine-grained sediment. The presence of sympagic nematodes has not yet been

confirmed in any sediment samples (Riemann and Sime-Ngando 1997), which agrees with the findings from the cruise in autumn 2018. No nematodes of similar morphology or molecular structure were found in the sediment in Van Mijenfjorden either. However, this might be a sampling artifact, as the smallest sized sieve used had a mesh size of 63 rather than 20 μm .

5.3 Sympagic-pelagic coupling in Van Mijenfjorden

Sympagic-pelagic coupling appeared to be rather weak in Van Mijenfjorden, in terms of faunal overlap between the sea ice and water column. The dominant sympagic meiofauna was sparsely recorded from the net sample, which yielded higher numbers of copepods than the sea ice samples. It is not possible to extrapolate from the data wherein the water column the zooplankton was located. However, it could be speculated that various groups of the fauna identified must be situated close to the ice-water interface, as this is where the highest concentration of ice algal biomass is located. A few of the copepods recorded from net samples were found in the lower 0–1 cm of the ice. At the start of the spring season, ice algal concentrations exceed those of phytoplankton by several orders of magnitude (e.g. Grainger and Hsiao 1990; this study), thus making the underside and inside of the ice a potential feeding site. Copepods of the order Harpacticoida and Cyclopoida are frequently observed near or at the ice-water interface in spring to feed (e.g. Grainger and Hsiao 1990) and representative genera of these orders were observed in samples in Van Mijenfjorden (e.g. *Triconia* spp.). Similarly to sympagic meiofauna, microzooplankton can utilize ice algae to fuel reproduction, ensuring eggs are laid and nauplii are hatching when food is abundant in the water column (e.g. Søreide et al. 2010; Jia et al. 2016). Considering the variety of eggs and the presence of nauplii, both in ice and water samples, in Van Mijenfjorden, this seems like a valid assumption.

5.4 Molecular identification of nematodes

Genetic analysis of individual sympagic nematodes revealed the potential for *Halomonhystera* sp. to inhabit the landfast ice in Van Mijenfjorden. *Halomonhystera* is a well-known genus from the intertidal zone (Andrássy 2006; Derycke et al. 2007; Van Campenhout et al. 2014), the White Sea and mud volcanoes in the Arctic Ocean (Tchesunov et al. 2015). The genus belongs to the family Monhysteridae and forms a larger complex of cryptic species, which vary in morphology,

but overlap within one species (due to selection and environmental pressure) is not uncommon (e.g. Derycke et al. 2007a; Tchesunov et al. 2015).

The sequences obtained from the Svalbard specimens did not cluster directly with any of the lineages available in *NCBI/GenBank*, which indicates either the presence of a new species or a solely morphologically identified nematode with no available sequences. Considering how sparse the molecular database is, this seems like a valid assumption.

Since the mid-1990's no new sympagic nematodes have been described – neither morphologically nor molecularly, and none of the three known species has been sequenced (see Tchesunov 1986; Tchesunov and Riemann 1995). One of the endemic sympagic species described was *Theristus melnikovi* (Tchesunov 1986), which is a close relative of *Theristus acer* (Tchesunov and Riemann 1995). Therefore, it would be intriguing to morphologically examine individual nematodes found in the ice in Wahlenbergfjorden to investigate whether the molecular results are correct in assuming that the sequenced individual is *T.acer* or could potentially represent the ice-endemic nematode *T.melnikovi*. Considering the north-easterly location of Wahlenbergfjorden and its close proximity to Hinlopen Strait, through which pack ice is transported, the latter option cannot be disregarded.

Mitochondrial rather than nuclear DNA was used in this study due to the availability of specific 18S rDNA primers (e.g. Bhadury et al. 2005), as COI genetic markers for free-living nematodes are not readily available (Derycke et al. 2010b). Although the use of COI is preferred for sequencing metazoans, as 18S rDNA tends to provide low resolution on the species level (Derycke et al. 2010b; Macheriotou et al. 2019), numerous studies have shown that the use of specific 18s rDNA primers is successful at identifying nematodes to genus level (e.g. Bhadury et al. 2005; 2006). In addition, 18S rDNA sequences offer the most available, though far from complete, database (Bik 2010). Therefore, the use of nematode-specific primers that target highly conserved regions within small sub-unit genes, as in this study, is a good starting point for identifying unknown specimen (Bik 2010). However, in future it would be advantageous to use both specific 18S rDNA primers and markers for the COI gene to obtain as much molecular taxonomic information as possible, and to allow comparison between the different methods (e.g. Tchesunov et al. 2015).

6. Uncertainties and future work

There are several uncertainties associated with this project. Should this study be repeated in future the following points should be taken into consideration. Nevertheless, this project reveals interesting findings about sympagic meiofaunal abundance and activity in Van Mijenfjorden, Svalbard.

Firstly, there are uncertainties associated with the sea ice samples. It cannot be guaranteed that the ice cores were cut as accurately as the sectioning that was selected (0-1, 1-2, 2-3 cm). Although two people were working at the same time, the saw had a tendency to slip on the harder ice and it was difficult getting a good grip at the start. Additionally, when the ice was very brittle or soft, pieces from the adjacent section fell off.

Due to the identifiers lack of experience with ciliates, various organisms in the ‘unidentified’ fraction from the start of sampling campaign, might be unidentified ciliates, which are protozoa and not metazoan. Thus, the abundance of the unidentified fraction should be considered with caution.

Unfortunately, not all net samples collected alongside sea ice cores were included. At the time of analysis, a few of the samples had become opaque and “gloopy” making it not possible to pass them through a 20 µm sieve and reliably identify the microzooplankton present.

One of the environmental parameters that was not included in this study is light or PAR. Measurements were taken in the field, but the data were not seen as reliable and therefore not included. However, from the literature it is known, that light can be a driving factor in structuring sympagic communities. Therefore, it should be ensured that when collecting ice cores that reliable and consistent light measurements are taken to include them in the evaluation of the biotic data.

In future, a multi-variant analysis should be used to examine what environmental variables might be driving sympagic meiofauna patters between stations. In this study, a basic Spearman’s correlation test was used, but only five to six data points were included due to the simplicity of the test. Thus, the lack of significant correlations might be an artifact of small sample size and should be considered with caution. However, using a stronger statistical analysis might reveal trends known from other studies.

For the polychaete growth experiment evaluation, the number of setiger rather than length was used. Body length was not used as an indicator of growth, as the measurements from some treatments did not seem reliable. More often than not, polychaete juveniles were elongated or contracted, which means that on certain dates it seems that individuals in the control treatment grew the same as the specimens in the high food concentration. Therefore, I decided setiger number as an indication of growth rather than body length after Qian and Chia (1991). Therefore, it was not possible to calculate daily growth rate in each of the food treatments. Figure B2b shows the mean length of juvenile polychaetes from the experiment. This graph was included to allow direct comparison to the *in situ* measurements, as the number of setiger was not counted for the polychaete juveniles in the ice samples. However, those mean lengths should be considered with caution and for the evaluation of the experiment in this study, the setiger number should be used. Should the growth experiment be repeated, it would be better to use a chemical compound to narcotize the polychaetes, e.g. magnesium chloride (e.g. Yokoyama 1988). Additionally, it would be best to have a feeding replenishment event every third day. It was observed during this experiment that juvenile polychaetes appeared more sluggish and less intensively coloured when the water was changed on the fourth and fifth day rather than the third day. This is pointing to potential starvation, which can be avoided by replenishment on shorter time intervals.

For future molecular work, it would be advantageous to use both 18S rDNA and the COI gene. This would enable more in-depth comparison with the available literature and might provide more hits in the *NCBI/GenBank* databases, as well as better insight into divergence of lineages. It would also be advantageous to study the morphology of the collected nematodes in greater detail than it has been in this study. Only size measurements were taken for this project, which are useful to track reproduction and the appearance of juvenile. However, distinction between male and females (based on the structure and positioning of reproductive organs) are needed to assign size classes to species. This would allow for morphological comparison with published literature (e.g. Tchesunov 1986; Tchesunov et al. 2015) and add valuable information that could be used in evaluating the molecular data.

Additionally, rather than preserving individual specimens in ethanol, it would be better to place them with as little liquid as possible in an Eppendorf tube (Eppendorf, Germany), after rinsing, and freezing them at -80°C . This would reduce the number of steps in-between

preservation and DNA extraction, and ultimately decrease the chance of losing the individual. This would be especially important with the juvenile nematodes, which are very small (< 1700 µm) and have a tendency to stick to the bottom of the petri dish, used for pre-extraction rinsing, and dissolve.

7. Conclusion and outlook

This study has provided insights into the seasonal development and activity of sympagic meiofauna in Van Mijenfjorden, Svalbard. The data showed that not only was there a difference in sympagic meiofauna abundance due to temporal variability, but also over a spatial scale due to differences in water depth and subsequently, the strength of sympagic-pelagic-benthic coupling. Similarly to other regions of the Arctic, benthic fauna abundance in the ice decreased with increasing water depth. Ice nematodes appeared to be using the sea ice, over deeper water (> 50 m), as a reproductive ground with the appearance of sexually mature nematodes, eggs and juveniles in late spring. Comparatively, sea ice served as a nursery ground for juvenile polychaetes, over the shallowest stations (2 to 15 m), which utilized ice algae to fuel their growth and development before returning to the seafloor.

The data collected confirmed that Svalbard ice meiofauna changes are similar to the patterns seen in other parts of the Arctic. However, rather than using coarse taxonomic resolution, this study tried to identify the two dominant sympagic meiofauna (nematodes and juvenile polychaetes) to genus level. Although morphological validation is needed to confirm the molecular findings for ice nematodes, it did provide valuable information and opened the door for new research questions, as discussed for nematodes. Such specific information is needed, as with changing ice conditions, changes in the species utilizing Svalbard landfast ice throughout the spring could occur otherwise undetected. Various sympagic meiofaunal groups, such as nematodes and polychaetes, have important ecological functions. Consequently, it is of uttermost importance to identify organisms in the sea ice to the lowest taxonomic level possible to see how their recruitment success might be affected by changing ice conditions and to examine what role they play in the rest of the Arctic coastal ecosystem. This information is valuable in accessing how higher trophic levels might respond should there be a shift in species and sympagic-pelagic-benthic coupling. While the growth experiment did provide some insights into the feed

concentration effects on growth of ice polychaetes, similar approaches should also be used to increase our knowledge on sympagic food webs in general.

Appendix A

This appendix contains supplementary information for the materials and methods section.

Table A1. Information about the easterly sampling stations on Svalbard. SM = Sympagic meiofauna; N/A = Not available.

Date [YYYY-MM-DD]	Latitude [Decimal degrees]	Longitude [Decimal degrees]	Location	Station ID	Depth [m]	Sample
May 2015	79.6667	20.0000	Wahlenbergfjorden, Nordauslandet	WB	N/A	SM
2018-03-22	77.8758	18.27045	Inglefieldbukta, east Spitsbergen	IB1	2 - 4	SM
2018-03-23	77.89088	18.23837	Inglefieldbukta, east Spitsbergen	IB2	30	SM
2018-04-26	77.88758	18.27045	Inglefieldbukta, East Spitsbergen	IB1	2 - 4	SM
2018-06-18	79.57372	20.66888	Palanderbukta, Nordauslandet	PAL	18	SM

Table A2. Station and equipment information from the cruise with *MS Polarsysssel*, in Van Mijenfjorden in November 2018. N/A = Not available.

Date [YYY Y-MM-DD]	Station	Station ID	Latitude [Decimal degrees]	Longitude [Decimal degrees]	Depth [m]	Equipment	Sample depth [m]	Equipment	Sample depth [m]
2018-11-14	vMF1	Stn C	77.82528	16.61783	79	Grab	79	20 µm net	70
2018-11-14	vMF	Stn B	77.86017	16.70978	41	Grab	41	20 µm net	31
2018-11-14	vMF30	Stn A	77.86325	16.73212	32	Grab	32	20 µm net	25
2018-11-14	vMF/Ref	Stn X	77.884533	16.7305	0.8-1	Grab	0.8-1	N/A	N/A

Table A3. Feed concentrations used during the polychaete growth experiment.

Preparation date	Sample ID	Cell abundance (mL ⁻¹)	Volume added (µL ⁻¹)
07.04.2018	Low	N/A	N/A
	Medium	N/A	N/A
	High	N/A	N/A
11.04.2018	Low	3	5
	Medium	100	19.5
	High	30,000	1,000
13.04.2018	Low	3	5
	Medium	100	19.5
	High	30,000	1,000
21.04.2018	Low	3	0.2
	Medium	100	6.7

	High	30,000	2,000
26.04.2018	Low	6	0.34
	Medium	100	11.1
30.04.2018	High	30,000	3,500
	Low	6	0.51
	Medium	100	8.4
04.05.2018	High	30,000	2,500
	Low	6	0.4
	Medium	100	6.7
09.05.2018	High	30,000	2,000
	Low	6	0.4
	Medium	100	6.7
13.05.2018	High	30,000	2,000
	Low	6	0.23
	Medium	100	7.6
16.05.2018	High	30,000	2,300
	Low	6	0.34
	Medium	100	5.7
21.05.2018	High	30,000	1,700
	Low	N/A	N/A
	Medium	N/A	N/A
	High	N/A	N/A

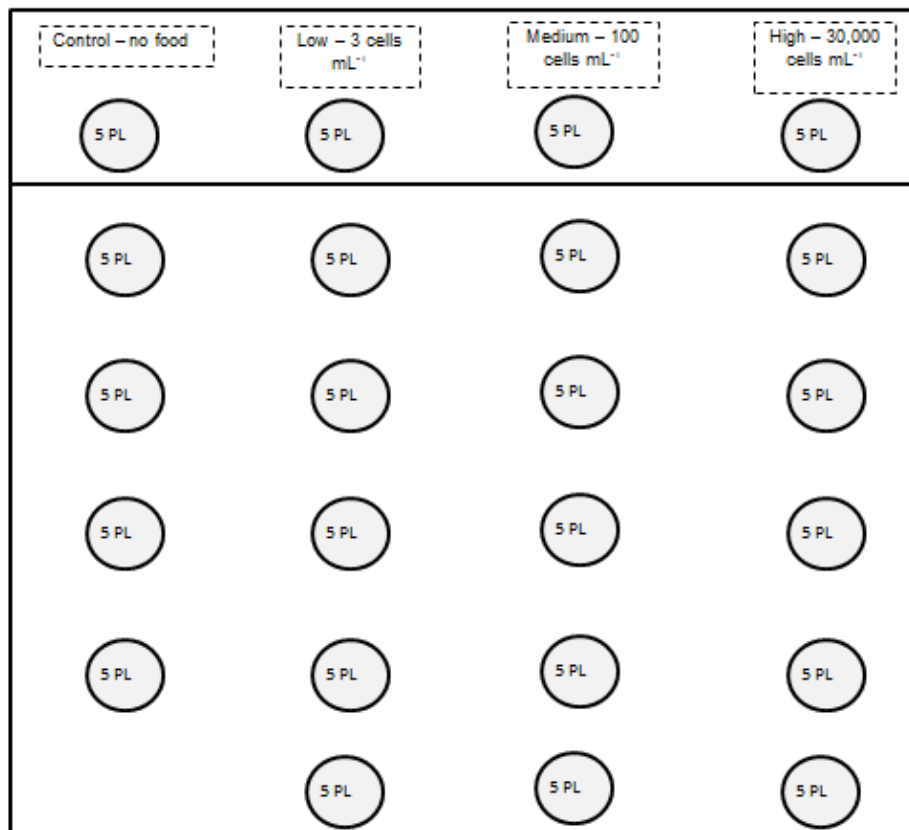


Figure A1. Set-up of polychaete juvenile growth experiment with four different food concentrations and four to five replicates per treatment.

Table A4. Nematode sequences selected based on closest hit from *NCBI* BLAST and literature. N/A = Not available.

Nematode reference sequence	Accession number	Reference
<i>Geomonhystera disjuncta</i> partial 18S rRNA gene, from Netherlands, Westerschelde	AJ966485	Meldal et al. (2007)
<i>Halomonhystera</i> sp. JvC-2013 partial 18S rRNA gene, isolate MSM16-2_802-1	HF572952.2	Van Campenhout et al. (2014)
<i>Halomonhystera</i> sp. gd4 voucher Ugent_CeMoFeGG2339_18S small subunit ribosomal RNA gene, partial sequence	MG669808	Macheriotou et al. (2019)
<i>Halomonhystera</i> sp. gd4 voucher Ugent_CeMoFeGG2336_18S small subunit ribosomal RNA gene, partial sequence	MG669807	Macheriotou et al. (2019)
<i>Halomonhystera</i> sp. gd4 voucher Ugent_CeMoFeGG2332_18S small subunit ribosomal RNA gene, partial sequence	MG669806	Macheriotou et al. (2019)
<i>Halomonhystera</i> sp. gd4 voucher Ugent_CeMoFeGG2320_18S small subunit ribosomal RNA gene, partial sequence	MG669805	Macheriotou et al. (2019)
<i>Halomonhystera</i> sp. gd1 voucher Ugent_CeMoFeOG2273_18S small subunit ribosomal RNA gene, partial sequence	MG669800	Macheriotou et al. (2019)
<i>Halomonhystera</i> sp. gd1 voucher Ugent_CeMoFeOG2264_18S small subunit ribosomal RNA gene, partial sequence	MG669799	Macheriotou et al. (2019)
<i>Halomonhystera</i> sp. gd1 voucher Ugent_CeMoFeOG2261_18S small subunit ribosomal RNA gene, partial sequence	MG669798	Macheriotou et al. (2019)
<i>Halomonhystera</i> sp. gd2 voucher Ugent_CeMoFeYG2393_18S small subunit ribosomal RNA gene, partial sequence	MG669801	Macheriotou et al. (2019)
<i>Halomonhystera</i> sp. gd3 voucher Ugent_CeMoFeBLG2412_18S small subunit ribosomal RNA gene, partial sequence	MG669802	Macheriotou et al. (2019)
<i>Halomonhystera</i> sp. gd3 voucher Ugent_CeMoFeBLG2424_18S small subunit ribosomal RNA gene, partial sequence	MG669803	Macheriotou et al. (2019)
<i>Halomonhystera</i> sp. gd3 voucher Ugent_CeMoFeBLG2431_18S small subunit ribosomal RNA gene, partial sequence	MG669804	Macheriotou et al. (2019)
<i>Theristus acer</i> voucher	MG670060.1	Macheriotou et al. (2019)

Ugent_CeMoFe4C9M12_18S small subunit ribosomal RNA gene, partial sequenc		
<i>Theristus</i> sp. 1 LM-2017 voucher Ugent_CeMoFe2A7E12_18S small subunit ribosomal RNA gene, partial sequence	MG670070.1	Macheriotou et al. (2019)
<i>Theristus acer</i> voucher Ugent_CeMoFe2C9M12_18S small subunit ribosomal RNA gene, partial sequence	MG670059.1	Macheriotou et al. (2019)
<i>Theristus acer</i> partial 18S rRNA gene, isolated in Netherlands, Westerschelde	AJ966505.1	Meldal et al. (2007)
<i>Theristus acer</i> partial 18S rRNA gene, specimen voucher Warwick RM 178943 (Smithsonian National Musuem of Natural History)	AM234627.1	Bhadury et al. (2006)
<i>Theristus</i> sp. M1 18S ribosomal RNA gene, partial sequence	KX944166	Avo et al. (2017)
<i>Diplolaimella dievengatensis</i> partial 18S rRNA gene, specimen voucher Moens T. (Ghent)	AJ966482.1	After Tchesunov et al. (2015)
<i>Diplolaimella dievengatensis</i> partial 18S rRNA gene	AM748763.1	After Tchesunov et al. (2015)
GD 1 - 5	N/A	Derycke et al. (2007a)
HMMV	N/A	Tchesunov et al. (2015)

Appendix B

This appendix contains supplementary information for the results section.

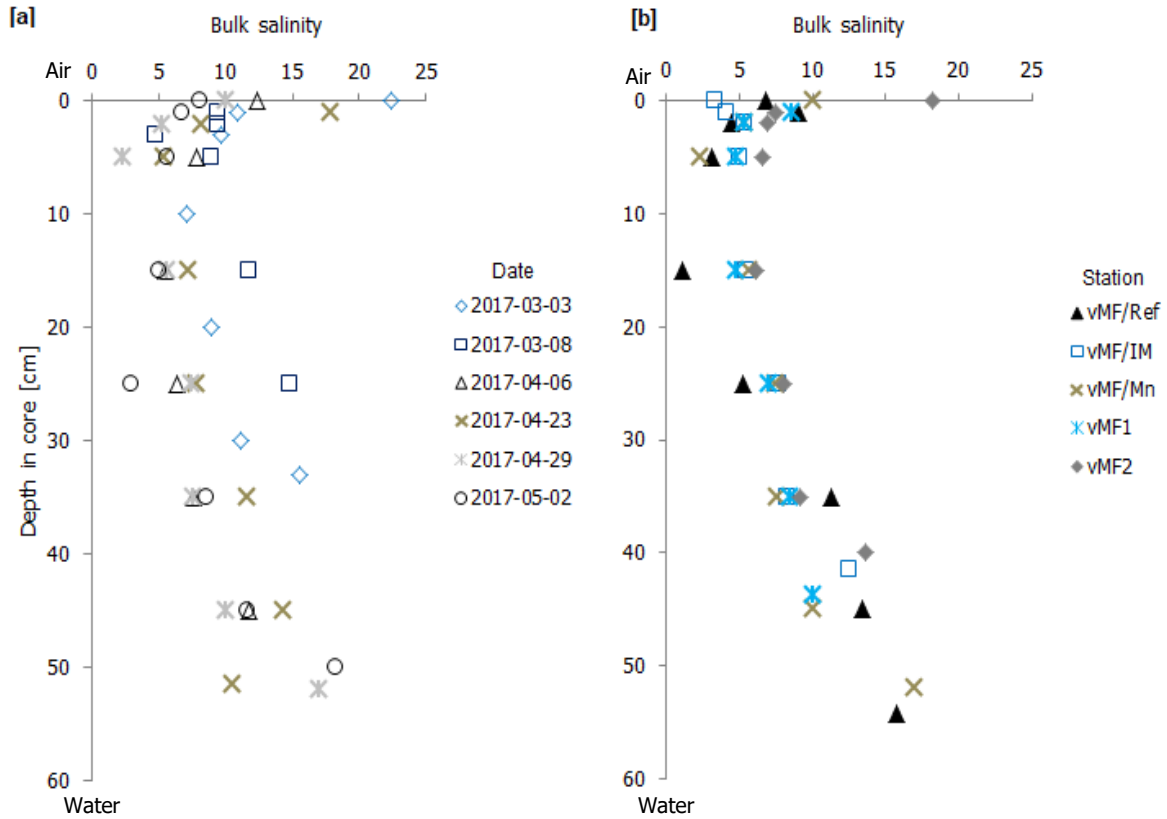


Figure B1. Bulk salinity measured for [a] all dates at station vMF/Mn and [b] all transect stations (26 to 30 April).

Table B1. Spearman's correlation test between sympagic meiofauna, abiotic and biotic variables in the lowermost 10 cm of the ice, with significance set at $p < 0.05$. Results are displayed with the Rho value first followed by the p -value in parentheses. SM = Sympagic meiofauna; N/A = Not available.

Data series	Organism	Chl a	WD	SA	JD
Transect	Nematodes	0.700 (0.188)	-0.100 (0.873)	0.616 (0.269)	N/A
Transect	Polychaetes	-0.103 (0.870)	-0.872 (0.05)	-0.158 (0.800)	N/A
Transect	Bulk SM	0.400 (0.505)	-0.500 (0.391)	0.359 (0.553)	N/A
Main station	Nematodes	0.429 (0.397)	N/A	0.086 (0.872)	0.0857 (0.872)
Main station	Polychaetes	-0.429 (0.397)	N/A	-0.314 (0.544)	-0.314 (0.544)
Main station	Bulk SM	0.149 (0.787)	N/A	-0.086 (0.872)	-0.086 (0.872)

Table B2. Abundance of zooplankton (ind m⁻²) in 20 µm net samples from Van Mijenfjorden.

Date	03 March	23 March	26 April
Station			
Organisms (ind m ⁻²)	vMF/Mn	vMF/Mn	vMF2
Nematode	107.7	102.6	0.00
Polychaete juvenile	0.00	153.9	13.7
Trochophore larvae	30.8	897.4	13.7
Nauplii	476.9	1718.0	1071.4
Cirripede nauplii	0.00	9794.9	2568.7
Egg	230.8	256.4	109.9
<i>Oithona</i> spp.	246.2	538.5	315.9
<i>Triconia</i> spp.	123.1	410.3	68.7
<i>Pseudocalanus</i> spp.	476.9	1692.3	123.6
<i>Acartia longiremis</i>	15.4	0.00	0.00
<i>Microsetella norvegica</i>	0.00	102.6	13.7
Small Calanus spp.	0.00	51.3	0.00
Chaetognath	30.8	0.00	13.7
Cnidarian	0.00	25.6	0.00
Unidentified	61.5	76.9	13.7

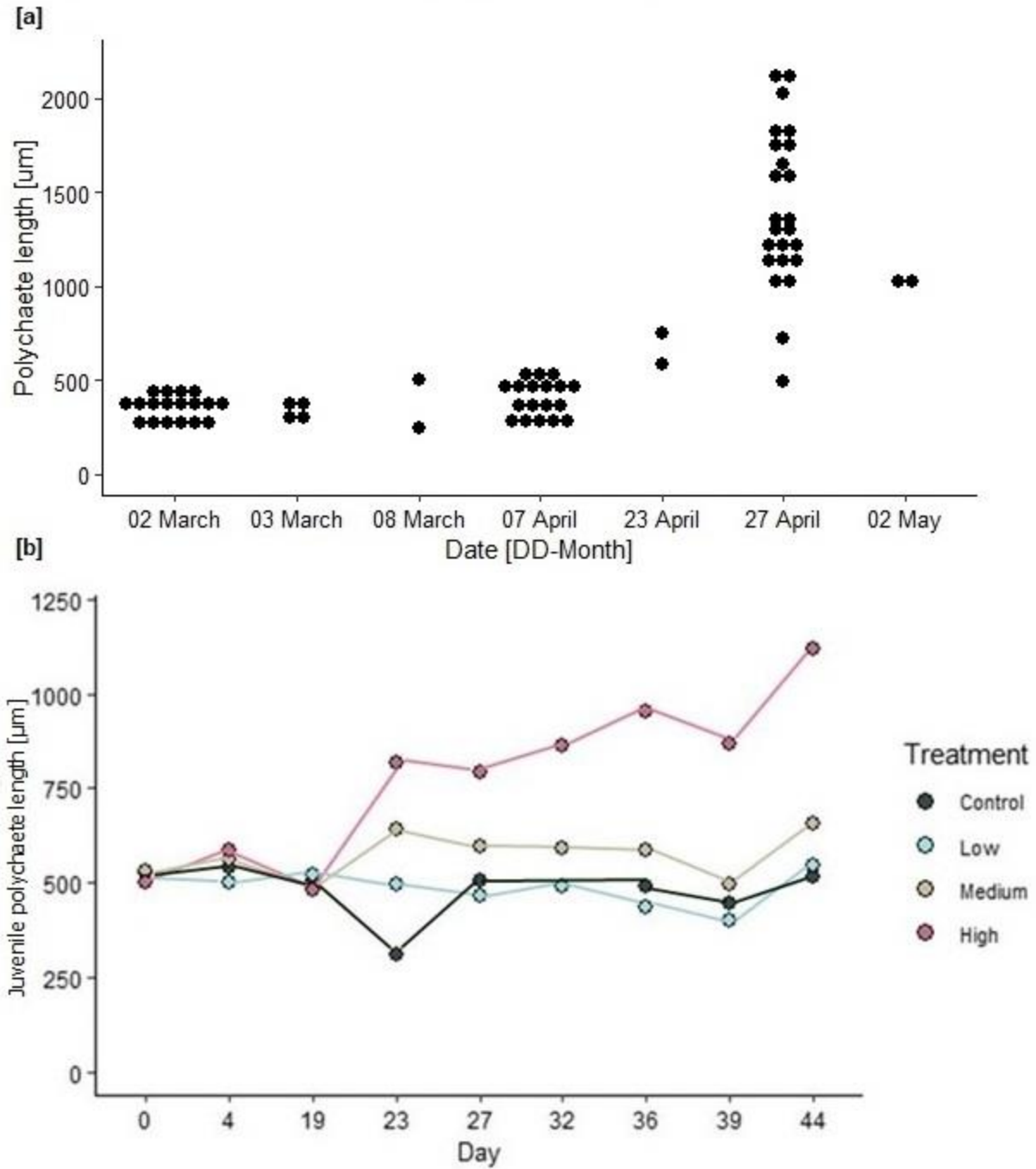


Figure B2. [a] *in situ* juvenile polychaete measurements (µm) and [b] mean length of polychaete juveniles in each food treatment over the duration of the growth experiment.

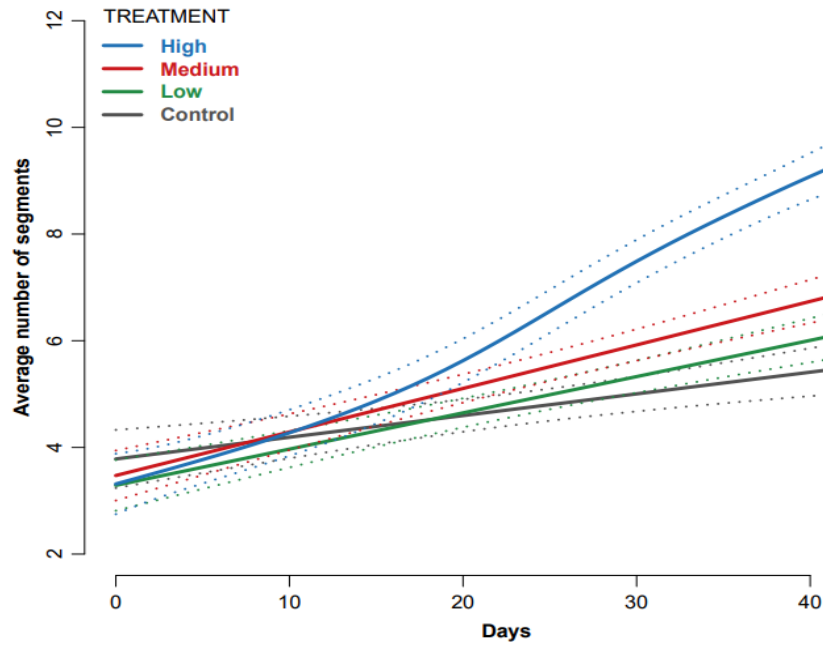


Figure B3. Generalized Additive Mixed Model output for the polychaete juvenile growth experiment.

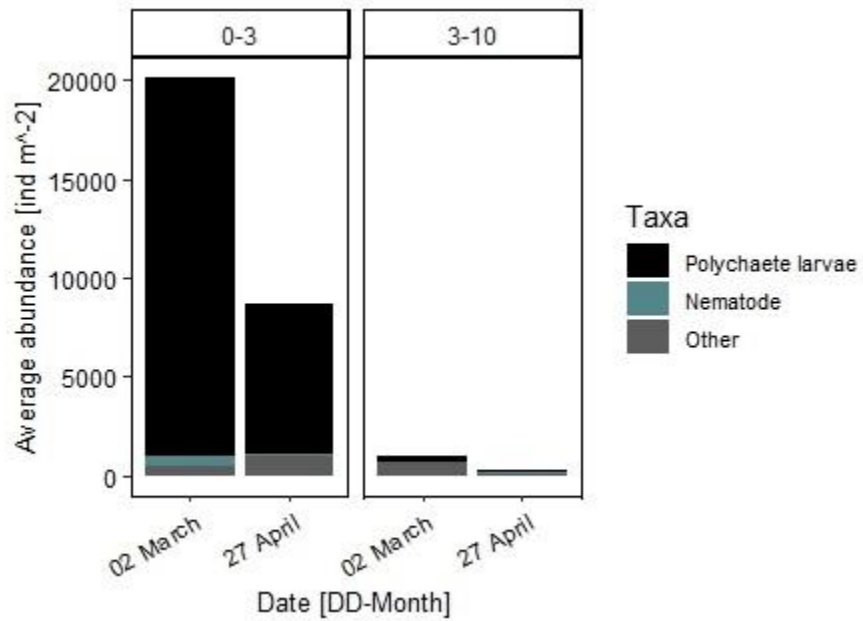


Figure B4. Integrated sympagic meiofauna abundance of the three most abundant fractions at station vMF/Ref within the lowermost 10 cm of the sea ice.

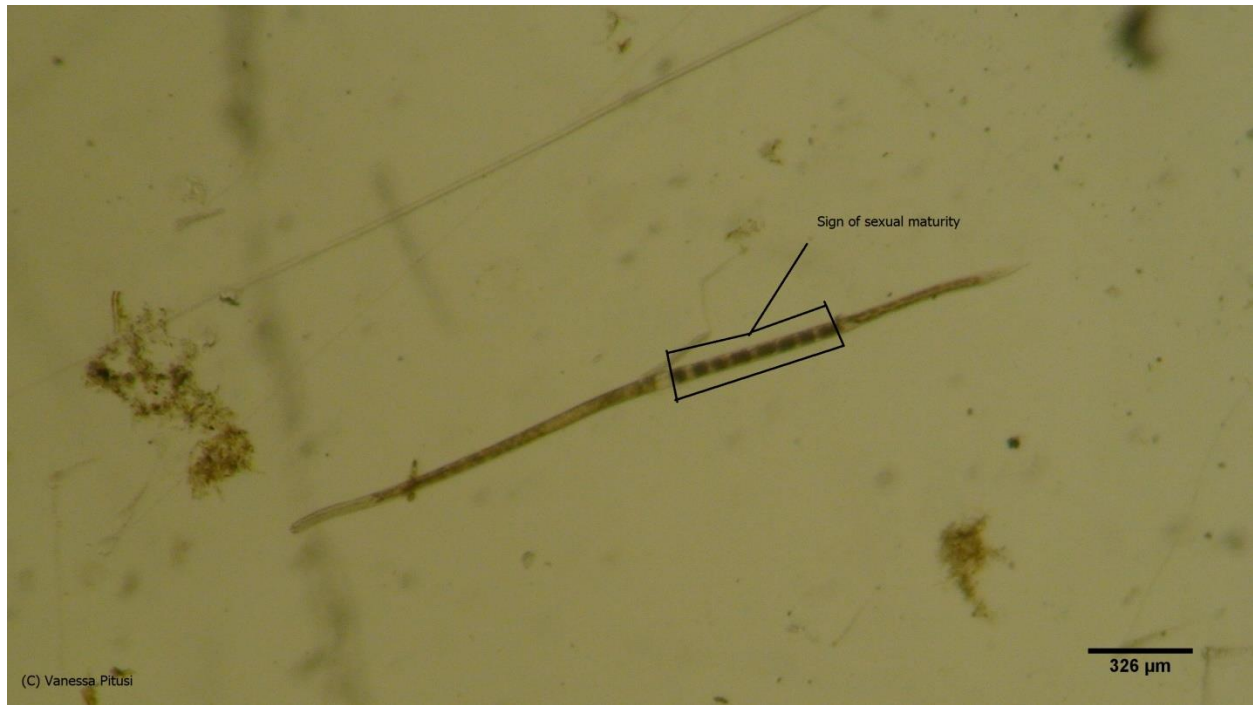


Figure B5. Sexually mature nematode found in sea ice sample at station vMF/Mn in late April 2017.

Table B3. Successfully sequenced sympagic juvenile polychaetes and their respective hits in the *NCBI/GenBank* database.

Date	Station	Sample	BLAST hit	Query cover	ID
17.04.2018	vMF30	Qualitative	Spionidae sp.	93 %	97 %
17.04.2018	vMF30	Qualitative	Spionidae sp.	97 %	97 %
17.04.2018	vMF30	Qualitative	Spionidae sp.	99 %	97 %
17.04.2018	vMF30	Qualitative	Spionidae sp.	97 %	96 %
17.04.2018	vMF30	Qualitative	Spionidae sp.	94 %	97 %
17.04.2018	vMF30	Qualitative	Spionidae sp.	94 %	97 %
17.04.2018	vMF30	Qualitative	Spionidae sp.	95 %	97 %

Bibliography

- Alasaad S, Rossi L, Maione S, Sartore S, Soriguer RC, Pérez JM, Rasero R, Zhu XQ, Soglia D (2008) HotSHOT Plus ThermalSHOCK, a new and efficient technique for preparation of PCR-quality mite genomic DNA. *J PARASITOL RES* 103:1455
- Andrássy I (2006) *Halomonhystera*, a new genus distinct from *Geomonhystera* Andrásy, 1981 (Nematoda: Monhysteridae). *MEIOFAUNA MARINA* 15:11-24
- Assmy P, Fernández-Méndez M, Duarte P, Meyer A, Randelhoff A, Mundy CJ, Olsen LM, Kauko HM, Bailey A, Chierici M, Cohen L (2017) Leads in Arctic pack ice enable early phytoplankton blooms below snow-covered sea ice. *SCI REP* 7:40850
- Arrigo KR, Perovich DK, Pickart RS, Brown ZW, Van Dijken GL, Lowry KE, Mills MM, Palmer MA, Balch WM, Bahr F, Bates NR (2012) Massive phytoplankton blooms under Arctic sea ice. *SCIENCE* 336:1408-1408
- Avó AP, Daniell TJ, Neilson R, Oliveira S, Branco J, Adão H (2017) DNA barcoding and morphological identification of benthic nematodes assemblages of estuarine intertidal sediments: advances in molecular tools for biodiversity assessment. *FRONT MAR SCI* 4:66
- Berge J, Cottier F, Varpe O, Renaud PE, Falk-Petersen S, Kwasniewski S, Majaneva S (2014) Arctic complexity: a case study on diel vertical migration of zooplankton. *J PLANKTON RES* 36:1279-1297
- Bhadury P, Austen MC, Bilton DT, Lamshead PJ, Rogers AD, Smerdon GR (2005) Combined morphological and molecular analysis of individual nematodes through short-term preservation in formalin. *MOL ECOL NOTES* 5:965-968
- Bhadury P, Austen MC, Bilton DT, Lamshead PJ, Rogers AD, Smerdon GR (2006) Development and evaluation of a DNA-barcoding approach for the rapid identification of nematodes. *MAR ECOL PROG SER* 320:1-9
- Bik HM (2010) Resolving phylogenetic relationships within the order Enoplida (Phylum Nematoda). Dissertation, National Oceanography Centre, Southampton

- Bluhm BA, Gradinger R, Piraino S (2007) First record of sympagic hydroids (Hydrozoa, Cnidaria) in Arctic coastal fast ice. *POLAR BIOL* 30:1557-1563
- Bluhm BA, Hop H, Melnikov IA, Poulin M, Vihtakari M, Collins ER, Gradinger R, Juul-Pedersen T, von Quillfeldt C (2017) Sea Ice Biota. In: SAMBR scientific report, pp 33 - 58
- Bluhm BA, Hop H, Vihtakari M, Gradinger R, Iken K, Melnikov IA, Søreide JE (2018) Sea ice meiofauna distribution on local to pan-Arctic scales. *ECOL EVOL* 8:2350-2364
- Brandner MM, Stübner E, Reed AJ, Gabrielsen TM, Thatje S (2016) Seasonality of bivalve larvae within a high Arctic fjord. *POLAR BIOL* 40:263-276
- Carey AG Jr, Montagna PA (1982) Arctic sea ice faunal assemblage: first approach to description and source of the underice meiofauna. *MAR ECOL PROG SER* 8:1-8
- Chauhan T, Rasmussen TL, Noormets R, Jakobsson M, Hogan KA (2014) Glacial history and paleoceanography of the southern Yermak Plateau since 132 ka BP. *QUAT SCI REV* 92:155–169
- Comiso JC, Parkinson CL, Gersten R, Stock L (2008) Accelerated decline in the Arctic sea ice cover. *GEOPHYS RES LETT* 35
- Comiso JC (2012) Large decadal decline of the Arctic multiyear ice cover. *J CLIMATE* 25:1176-1193
- Cottier F, Tverberg V, Inall M, Svendsen H, Nilsen F, Griffiths C (2005) Water mass modification in an Arctic fjord through cross-shelf exchange: The seasonal hydrography of Kongsfjorden, Svalbard. *J GEOPHYS RES OCEAN* 110:1–18
- Cox GFN, Weeks WF (1983) Equations for determining the gas and brine volume in sea-ice samples. *J GLACIOL* 29:306-316
- Daase M, Falk-Petersen S, Varpe Ø, Darnis G, Søreide JE, Wold A, Leu E, Berge J, Philippe B, Fortier L (2013) Timing of reproductive events in the marine copepod *Calanus glacialis*: a pan-Arctic perspective. *CAN J FISH AQUAT SCI* 70:871-884

- Dauer DM (1983) Functional morphology and feeding behavior of *Scolecopsis squamata* (Polychaeta: Spionidae). MAR BIOL 77:279-285
- De Mesel I, Derycke S, Swings J, Vincx M, Moens T (2006) Role of nematodes in decomposition processes: Does within-trophic group diversity matter?. MAR ECOL PROG SER 321:157-166
- Deming JW, Collins RE (2017) Sea ice as a habitat for Bacteria, Archaea and Viruses. In: Sea Ice, 3rd Edition, Editor Thomas DN, Wiley Blackwell, USA, pp 326 - 351
- Derycke S, Backeljau T, Vlaeminck C, Vierstraete A, Vanfleteren J, Vincx M, Moens T (2007a) Spatiotemporal analysis of population genetic structure in *Geomonhystera disjuncta* (Nematoda, Monhysteridae) reveals high levels of molecular diversity. MAR BIOL 151:1799-1812
- Derycke S, De Ley P, Tandingan De Ley I, Holovachov O, Rigaux A, Moens T (2010a) Linking DNA sequences to morphology: cryptic diversity and population genetic structure in the marine nematode *Thoracostoma trachygaster* (Nematoda, Leptosomatidae). ZOOL SCR 39:276-289
- Derycke S, Vanaverbeke J, Rigaux A, Backeljau T, Moens T (2010b) Exploring the use of cytochrome oxidase c subunit 1 (COI) for DNA barcoding of free-living marine nematodes. PLoS One 5:e13716
- Eamer J, Donaldson GM, Gaston AJ, Kosobokova KN, Larusson KF, Melnikov IA, Reist JD, Richardson E, Staples L, von Quillfeldt CH (2013) Life Linked to Ice: A guide to sea-ice-associated biodiversity in this time of rapid change. CAFF ASSESSMENT SERIES NO. 10, Conservation of Arctic Flora and Fauna, Iceland
- Eberhard S, Finazzi G, Wollman FA (2008) The dynamics of photosynthesis. ANNU REV GENET 42:463-515
- Edgar RC (2004) MUSCLE: a multiple sequence alignment method with reduced time and space complexity. BMC BIOINFORMATICS 5:113
- FinchTV 1.5.0. Geospiza, Inc., Seattle, WA, USA. Available from: <http://www.geospiza.com>

- Fonseca G, Decraemer W (2008) State of the art of the free-living marine Monhysteridae (Nematoda). *J MAR BIOL ASSOC UK* 88:1371-1390
- Friedrich C (1997) *Ökologische Untersuchungen zur Fauna des arktischen Meereises*. Dissertation, University of Kiel
- Garrison DL, Buck KR (1986) Organism losses during ice melting: a serious bias in sea ice community studies. *POLAR BIOL* 6:237-239
- Geneious V 11.0.4. Biomatters Ltd., New Zealand. Available from: <https://www.geneious.com>
- Gjelten HM, Nordli Ø, Isaksen K, Førland EJ, Sviashchennikov PN, Wyszynski P, Prokhorova UV, Przybylak R, Ivanov BV, Urazgildeeva AV (2016) Air temperature variations and gradients along the coast and fjords of western Spitsbergen. *POLAR* 35:29878
- Gradinger R (1999a) Vertical fine structure of the biomass and composition of algal communities in Arctic pack ice. *MAR BIOL* 133:745-754
- Gradinger R (1999b) Integrated abundance and biomass of sympagic meiofauna in Arctic and Antarctic pack ice. *POLAR BIOL* 22:169-177
- Gradinger R, Kaufman M, Bluhm B (2009) Pivotal role of sea ice sediments in the seasonal development of near-shore Arctic fast ice biota. *MAR ECOL PROG SER* 394:49-63
- Grainger EH, Mohammed AA (1990) High salinity tolerance in sea ice copepods. *OPHELIA* 31:177-185
- Grainger EH, Hsiao SI (1990) Trophic relationships of the sea ice meiofauna in Frobisher Bay, Arctic Canada. *POLAR BIOL* 10:283-292
- Gulliksen B, Lønne OJ (1991) Sea ice macrofauna in the Antarctic and the Arctic. *J MAR SYST* 2:53-61
- Heip C, Vincx M, Vranken G (1985) *The ecology of marine nematodes*. Aberdeen University Press

- Horner RA, Schrader GC (1982) Relative contributions of ice algae, phytoplankton, and benthic microalgae to primary production in nearshore regions of the Beaufort Sea. *ARCTIC* 485-503
- Horner R, Ackley SF, Dieckmann GS, Gulliksen B, Hoshiai T, Legendre L, Melnikov IA, Reeburgh WS, Spindler M, Sullivan CW (1992) Ecology of sea ice biota. *POLAR BIOL* 12:417-27
- Høyland KV (2009) Ice thickness, growth and salinity in Van Mijenfjorden, Svalbard, Norway. *POLAR RES* 28:339–352
- Hunt Jr GL, Drinkwater KF, Arrigo K, Berge J, Daly KL, Danielson S, Daase M, Hop H, Isla E, Karnovsky N, Laidre K (2016) Advection in polar and sub-polar environments: Impacts on high latitude marine ecosystems. *PROG OCEANGR* 1:40-81
- Hurst N, Gould T, Harrington B (2019) Inkscape. Available from: <http://www.inkscape.org/>
- Isaksen K, Nordli Ø, Førland EJ, Łupikasza E, Eastwood S, Niedźwiedź T (2016) Recent warming on Spitsbergen - Influence of atmospheric circulation and sea ice cover. *J GEOPHYS RES ATMOS* 121:11-913
- Jensen P (1987) Feeding ecology of free-living aquatic nematodes. *MAR ECOL PROG SER* 35:187-196
- Jia Z, Swadling KM, Meiners KM, Kawaguchi S, Virtue P (2016) The zooplankton food web under East Antarctic pack ice—a stable isotope study. *DEEP SEA RES PART 2 TOP STUD OCEANOGR* 131:189-202
- Kimura M (1980) A simple method for estimating evolutionary rate of base substitutions through comparative studies of nucleotide sequences. *J MOL EVOL* 16:111-120
- Krembs C, Gradinger R, Spindler M (2000) Implications of brine channel geometry and surface area for the interaction of sympagic organisms in Arctic sea ice. *J EXP MAR BIOL ECOL* 243:55-80
- Kumar S, Stecher G, Tamura K (2016) MEGA7: Molecular Evolutionary Genetics Analysis Version 7.0 for Bigger Datasets, *MOL BIOL EVOL* 33:1870–1874

- Kvernvik AC (2018) Ecophysiological Response of Sea Ice Algae and Phytoplankton to a Changing Arctic. Dissertation, University in Tromsø
- Larink O, Westheide W (2011) Coastal Plankton: Photo Guide for European Seas. Pfeil Verlag, Germany
- Lee DL (2002) The Biology of Nematodes. CRC Press Taylor and Francis Group, New York, 1st edition, pp 61 – 72
- Leray M, Yang JY, Meyer CP, Mills SC, Agudelo N, Ranwez V, Boehm JT, Machida RJ (2013) A new versatile primer set targeting a short fragment of the mitochondrial COI region for metabarcoding metazoan diversity: application for characterizing coral reef fish gut contents. FRONT ZOOL 10:34
- Leu E, Wiktor J, Søreide JE, Berge J, Falk-Petersen S (2010) Increased irradiance reduces food quality of sea ice algae. MAR ECOL PROG SER 411:49-60
- Leu E, Søreide JE, Hessen DO, Falk-Petersen S, Berge J (2011) Consequences of changing sea-ice cover for primary and secondary producers in the European Arctic shelf seas: timing, quantity, and quality. PROG OCEANOGR 90:18-32
- Leu E, Mundy CJ, Assmy P, Campbell K, Gabrielsen TM, Gosselin M, Juul-Pedersen T, Gradinger R (2015) Arctic spring awakening—Steering principles behind the phenology of vernal ice algal blooms. PROG OCEANOGR 139:151-170
- Macheriotou L, Guilini K, Bezerra TN, Tytgat B, Nguyen DT, Phuong Nguyen TX, Noppe F, Armenteros M, Boufahja F, Rigaux A, Vanreusel A (2019) Metabarcoding free-living marine nematodes using curated 18S and CO1 reference sequence databases for species-level taxonomic assignments. ECOL EVOL 9:1211-1226
- Majdi N, Traunspurger W (2015) Free-living nematodes in the freshwater food web: a review. J NEMATOL 47:28
- Marquardt M, Kramer M, Carnat G, Werner I (2011). Vertical distribution of sympagic meiofauna in sea ice in the Canadian Beaufort Sea. POLAR BIOL 34:1887-1900

- Marquardt M, Majaneva S, Pitusi V, Søreide JE (2018) Pan-Arctic distribution of the hydrozoan *Sympagohydra tuuli*? First record in sea ice from Svalbard (European Arctic). POLAR BIOL 41:583-588
- Maykut (1985) The Ice Environment. In: Horner R Sea ice biota. CRC Press, Boca Raton, pp 21-82
- McConnell B, Gradinger R, Iken K, Bluhm BA (2012) Growth rates of arctic juvenile *Scoelepis squamata* (Polychaeta: Spionidae) isolated from Chukchi Sea fast ice. POLAR BIOL 35:1487-1494
- McMinn A, Gradinger R, Nomura D (2009) Biochemical properties of sea ice. In: Eicken H et al (Eds) Field Techniques for sea ice research, pp 259-282
- Meldal BH, Debenham NJ, De Ley P, De Ley IT, Vanfleteren JR, Vierstraete AR, Bert W, Borgonie G, Moens T, Tyler PA, Austen MC (2007) An improved molecular phylogeny of the Nematoda with special emphasis on marine taxa. MOL PHYLOGENET EVOL 42:622-636
- Michel C, Nielsen TG, Nozais C, Gosselin M (2002) Significance of sedimentation and grazing by ice micro- and meiofauna for carbon cycling in annual sea ice (northern Baffin Bay). AQUAT MICROB ECOL 30:57-68
- Moens T, Vincx M (1997) Observations on the feeding ecology of estuarine nematodes. J MAR BIOL ASSOC UK 77:211-227
- Muckenhuber S, Nilsen F, Korosov A, Sandven S (2016) Sea ice cover in Isfjorden and Hornsund, Svalbard (2000 – 2014) from remote sensing data. THE CRYOSPHERE 10:149-158
- Mundy CJ, Barber DG, Michel C (2005) Variability of snow and ice thermal, physical and optical properties pertinent to sea ice algae biomass during spring. J MARINE SYST 58: 107-120
- Nicolaus M, Katlein C, Maslanik J, Hendricks S (2012) Changes in Arctic sea ice result in increasing light transmittance and absorption. GEOPHYS RES LETT 39:L24501

- Nilsen F, Skogseth R, Vaardal-Lunde J, Inall M (2016) A simple shelf circulation model: Intrusion of Atlantic water on the West Spitsbergen shelf. *J PHYS OCEANOGR* 46:1209-1230
- NOAA (2019) March Northern Hemisphere Sea Ice Extent 1979 – 2019. Available from: <https://www.ncdc.noaa.gov/snow-and-ice/extent/sea-ice/N/9>
- Nordli Ø, Przybylak R, Ogilvie AE, Isaksen K (2014) Long-term temperature trends and variability on Spitsbergen: the extended Svalbard Airport temperature series, 1898–2012. *POLAR RES* 33:21349
- Peterson BJ, McClelland J, Curry R, Holmes RM, Walsh JE, Aagaard K (2006) Trajectory shifts in the Arctic and Subarctic Freshwater Cycle. *SCIENCE* 313:1061-1066
- Piraino S, Bluhm BA, Gradinger R, Boero F (2008) *Sympagohydra tuuli* gen. nov. and sp. nov.(Cnidaria: Hydrozoa) a cool hydroid from the Arctic sea ice. *J MAR BIOL ASSOC UK* 88:1637-1641
- Pitusi V (2016) Seasonal development of ice algal biomass and sympagic meiofauna in Van Mijenfjorden, Southwest Svalbard. Bachelor thesis, Scottish Association for Marine Science, Oban
- Qian PY, Chia FS (1991) Effects of food concentration on larval growth and development of two polychaete worms, *Capitella capitata* (Fabricius) and *Polydora ligni* Webster. *BULL MAR SCI* 48:477-484
- R Core Team (2017) R: A language and environment for statistical computing. R Foundation for Statistical Computing, Vienna, Austria. Available from: <https://www.R-project.org/>
- Rasband WS (1997 - 2018) ImageJ. U.S. National Institutes of Health, Bethesda, Maryland, USA. Available from: <https://imagej.nih.gov/ij/>
- Renaud PE, Riedel A, Michel C, Morata N, Gosselin M, Juul-Pedersen T, Chiuchiolo A (2007) Seasonal variation in benthic community oxygen demand: a response to an ice algal bloom in the Beaufort Sea, Canadian Arctic?. *J MARINE SYST* 67:1-12

- Renaud PE, Włodarska-Kowalczyk M, Trannum H, Holte B, Węśławski JM, Cochrane S, Dahle S, Gulliksen B (2007) Multidecadal stability of benthic community structure in a high-Arctic glacial fjord (Van Mijenfjord, Spitsbergen). POLAR BIOL 30:295-305
- Riemann F, Sime-Ngando T (1997) Note on sea-ice nematodes (Monhysteroidea) from Resolute Passage, Canadian high Arctic. POLAR BIOL 18:70-75
- Screen JA, Simmonds I (2010a) The central role of diminishing sea ice in recent Arctic temperature amplification. NATURE 464:1334
- Screen JA, Simmonds I (2012) Declining summer snowfall in the Arctic: Causes, impacts and feedbacks. CLIM DYNAM 38:2243-2256
- Souza JR, Borzone CA (2000) Population dynamics and secondary production of *Scolelepis squamata* (Polychaeta: Spionidae) in an exposed sandy beach of southern Brazil. BULL MAR SCI 221-233
- Søreide JE, Leu EV, Berge J, Graeve M, Falk-Petersen ST (2010) Timing of blooms, algal food quality and *Calanus glacialis* reproduction and growth in a changing Arctic. GLOB CHANGE BIOL 16:3154-3163
- Søreide JE, Carroll ML, Hop H, Ambrose Jr WG, Hegseth EN, Falk-Petersen S (2013) Sympagic-pelagic-benthic coupling in Arctic and Atlantic waters around Svalbard revealed by stable isotopic and fatty acid tracers. MAR BIOL RES 9:831-850
- Speybroeck J, Alsteens L, Vincx M, Degraer S (2007) Understanding the life of a sandy beach polychaete of functional importance—*Scolelepis squamata* (Polychaeta: Spionidae) on Belgian sandy beaches (northeastern Atlantic, North Sea). ESTUAR COAST SHELF SCI 74:109-118
- Spindler M, Dieckmann GS (1986) Distribution and abundance of the planktic foraminifer *Neogloboquadrina pachyderma* in sea ice of the Weddell Sea (Antarctica). POLAR BIOL 5:185-191
- Stroeve JC, Markus T, Boisvert L, Miller J, Barrett A (2014) Changes in Arctic melt season and implications for sea ice loss. GEOPHYS RES LETT 41:1216-1225

- Stübner EI, Søreide JE, Reigstad M, Marquardt M, Blachowiak-Samolyk K (2016) Year-round meroplankton dynamics in high-Arctic Svalbard. *J PLANKTON RES* 38:522-536
- Szymelfenig M, Kwaśniewski S, Węśławski JM (1995) Intertidal zone of Svalbard. *POLAR BIOL* 15:137-141
- Tchesunov AV (1986) A new free-living nematode connected with sea Arctic ice. *ZOOL ZH* 65:1782-1787
- Tchesunov AV, Portnova DA, Campenhout J (2015) Description of two free-living nematode species of *Halomonhystera* disjuncta complex (Nematoda: Monhysterida) from two peculiar habitats in the sea. *HELGOLAND MAR RES* 69:57
- Tchesunov AV, Riemann F (1995) Arctic sea ice nematodes (Monhysteroidea), with descriptions of *Cryonema crassum* gen. n., sp. n. and *C. tenue* sp. n. *NEMATOLOGICA* 41:35-50
- Timco GW, Frederking RM (1996) A review of sea ice density. *COLD REG SCI TECHNOL* 24:1-6
- Truett GE, Heeger P, Mynatt RL, Truett AA, Walker JA, Warman ML (2000) Preparation of PCR-quality mouse genomic DNA with hot sodium hydroxide and tris (HotSHOT). *BIOTECHNIQUES* 29:52-54
- Vader A, Marquardt M, Meshram AR, Gabrielsen TM (2014) Key Arctic phototrophs are widespread in the polar night. *POLAR BIOL* 38:13-21
- Van Campenhout J, Derycke S, Moens T, Vanreusel A (2014) Differences in life-histories refute ecological equivalence of cryptic species and provide clues to the origin of bathyal *Halomonhystera* (Nematoda). *PLoS ONE* 9:e111889
- Van Campenhout J, Derycke S, Tchesunov AV, Portnova D, Vanreusel A (2014) The dominant Håkon Mosby mud volcano nematode is genetically differentiated from its shallow-water relatives and shows genetic structure within the mud volcano. *J ZOOL SYST EVOL RES* 52:203–216

Vranken G (1987) An autecological study of free-living marine nematodes. ACAD ANAL-MEDED K ACAD BELG KL WET 49:73-97

Walsh JE, Johnson CM (1979) An analysis of Arctic sea ice fluctuations, 1953-77. J PHYS OCEANOGR 9:580-591

Wickham H (2009) ggplot2: Elegant Graphics for Data Analysis. Springer-Verlag, New York

Yokoyama H (1988) Effects of temperature on the feeding activity and growth rate of the spionid polychaete *Paraprionospio* sp.(form A). J EXP MAR BIOL ECOL 123:41-60